PHYSICAL REVIEW C **87**, 014338 (2013)

Chiral Fermi liquid approach to neutron matter

J. W. Holt,[1,2] N. Kaiser,[1] and W. Weise[1,3]
[1]*Physik Department, Technische Universität München, D-85747 Garching, Germany*
[2]*Physics Department, University of Washington, Seattle, Washington 98195, USA*
[3]*ECT*, Villa Tambosi, I-38123 Villazzano (TN), Italy*

(Received 24 September 2012; revised manuscript received 19 December 2012; published 28 January 2013)

We present a microscopic calculation of the complete quasiparticle interaction, including central as well as noncentral components, in neutron matter from high-precision two- and three-body forces derived within the framework of chiral effective-field theory. The contributions from two-nucleon forces are computed in many-body perturbation theory to first and second order (without any simplifying approximations). In addition we include the leading-order one-loop diagrams from the next-to next-to leading order (N^2LO) chiral three-nucleon force, which contribute to all Fermi liquid parameters except those associated with the center-of-mass tensor interaction. The relative-momentum dependence of the quasiparticle interaction is expanded in Legendre polynomials up to $L = 2$. Second-order Pauli blocking and medium polarization effects act coherently in specific channels; namely, for the Landau parameters f_1, h_0, and g_0, which results in a dramatic increase in the quasiparticle effective mass as well as a decrease in both the effective tensor force and the neutron matter spin susceptibility. For densities greater than about half the nuclear matter saturation density ρ_0, the contributions to the Fermi liquid parameters from the leading-order chiral three-nucleon force scale in all cases approximately linearly with the nucleon density. The largest effect of the three-nucleon force is to generate a strongly repulsive effective interaction in the isotropic spin-independent channel. We show that the leading-order chiral three-nucleon force leads to an increase in the spin susceptibility of neutron matter, but we observe no evidence for a ferromagnetic spin instability in the vicinity of the saturation density ρ_0. This work sets the foundation for future studies of neutron matter response to weak and electromagnetic probes with applications to neutron star structure and evolution.

DOI: 10.1103/PhysRevC.87.014338 PACS number(s): 21.65.Cd, 21.65.Mn

I. INTRODUCTION

In a series of recent articles [1,2], we revisited the Fermi liquid description of infinite nuclear matter in the context of modern two- and three-nucleon interactions derived within the framework of chiral effective-field theory. In these studies we limited our discussion to the central components of the quasiparticle interaction in a medium of spin-saturated symmetric nuclear matter characterized by the nucleon density $\rho = 2k_f^3/(3\pi^2)$. In the vicinity of the saturation density ρ_0, the central components of the quasiparticle interaction are strongly constrained by the properties of bulk nuclear matter and its low-energy excitations. In Refs. [1,2] it was found that microscopic calculations of the quasiparticle interaction within many-body perturbation theory yield an accurate description of the nuclear matter compressibility, isospin asymmetry energy, and spin-isospin response only with the inclusion of leading-order medium effects, which arise at second order in a perturbative calculation with two-body forces and at first order in a calculation with three-nucleon forces.

In the present paper we extend these calculations to pure neutron matter, which we treat as a normal (nonsuperfluid) Fermi liquid (the generalization of Fermi liquid theory to superfluid Fermi systems has been performed in Refs. [3–5]). Such a quasiparticle description has been used in previous works to understand neutrino emissivity in neutron stars [6–9] as well as the spin response of neutron star matter to strong magnetic fields [10–13]. In such calculations, the Landau parameters that characterize the quasiparticle interaction have been computed with microscopic two-body nuclear forces or with phenomenological Skyrme and Gogny effective interactions. Qualitative differences arise between the predictions of microscopic and phenomenological forces, particularly with respect to the possibility of bulk magnetization or even the existence of a spontaneous ferromagnetic phase transition of neutron matter at several times the nuclear matter saturation density [12,14,15]. As discussed in Sec. V, three-neutron forces give rise to Fermi liquid parameters that scale approximately linearly with the neutron density (at leading order), and one of the primary goals of the present work is to better understand the role of three-neutron correlations in describing the dynamical response of neutron matter to weak or electromagnetic probes.

Both the magnetic susceptibility of dense neutron matter as well as neutrino elastic scattering, absorption, and emission rates are sensitive to the inclusion of noncentral components of the quasiparticle interaction [8,9,11], which have been introduced in Refs. [16,17]. Such interactions include (in the long-wavelength approximation) the exchange tensor interaction, proportional to $S_{12}(\hat{q}) = 3\vec{\sigma}_1 \cdot \hat{q}\, \vec{\sigma}_2 \cdot \hat{q} - \vec{\sigma}_1 \cdot \vec{\sigma}_2$, which appears already in the free-space nucleon-nucleon potential where it is dominated by one-pion exchange, as well as center-of-mass tensor and cross-vector interactions proportional to $S_{12}(\hat{P})$ and $(\vec{\sigma}_1 \times \vec{\sigma}_2) \cdot (\hat{q} \times \hat{P})$, respectively. In these spin-dependent operators, $\vec{q} = \vec{p}_1 - \vec{p}_2$ is the relative momentum and $\vec{P} = \vec{p}_1 + \vec{p}_2$ the center-of-mass momentum of the two quasiparticles on the Fermi surface ($|\vec{p}_{1,2}| = k_f$).

When including effects of the medium in the form of loop integrals over the filled Fermi sea of neutrons, all noncentral interactions can be generated. In fact, the second-order contributions from two-body forces produce exchange tensor, center-of-mass tensor, and cross-vector interactions. Note that the spin-nonconserving cross-vector interaction can only be generated through polarization (particle-hole) corrections to the effective interaction and not by ladders [17]. To date there has been no study of three-nucleon force contributions to either the center-of-mass tensor or cross-vector interactions, while in Ref. [18] loop diagrams involving intermediate Δ-isobar excitations were analyzed and shown to generate an exchange tensor interaction in symmetric nuclear matter.

The present work sets the foundation for a systematic study of the role played by second-order corrections and three-nucleon forces in determining the noncentral components of the quasiparticle interaction. Their effect on neutron star structure and evolution will be studied in future work. We employ many-body perturbation theory and compute all contributions to the quasiparticle interaction for the case of two neutrons on the Fermi surface interacting in a background medium of pure neutron matter. We employ high-precision chiral two- and three-nucleon interactions whose unresolved short-distance components are encoded in a set of contact couplings proportional to low-energy constants fit to elastic nucleon-nucleon scattering phase shifts and properties of light nuclei [19–21]. To improve the convergence of the microscopic calculation of the quasiparticle interaction in many-body perturbation theory, we employ renormalization-group methods for integrating out momenta beyond the scale of $\Lambda \simeq 2.0$ fm^{-1}, which results in the nearly universal two-nucleon potential $V_{\text{low-k}}$ [22,23]. The contributions to the quasiparticle interaction from the leading-order chiral three-nucleon force (with scale-dependent low-energy constants) is computed to one-loop order.

The present paper is organized as follows: In Sec. II we give a brief review of Landau's theory of normal Fermi liquids and discuss the microscopic approach for computing the quasiparticle interaction. We then present a general method that can be applied to any free-space nucleon-nucleon force given in a partial-wave basis for extracting the scalar functions that multiply the various spin-dependent operators (namely, the central, spin-spin, exchange tensor, center-of-mass tensor, and cross-vector terms) occurring in the quasiparticle interaction. We then discuss the microscopic origin of the spin-nonconserving cross-vector interaction, which at second-order results exclusively from the interference of a two-body spin-orbit force with (in principle) any non-spin-orbit component in the free-space nucleon-nucleon interaction. In Sec. III we test the intricate (numerical) calculations of the second-order contributions to the quasiparticle interaction by means of model interactions that can be solved partially analytically. In Sec. IV we present analytical formulas for the Landau parameters of the quasiparticle interaction arising from the leading-order next-to next-to leading-order (N^{2}LO) chiral three-neutron force. The results of the corresponding calculations with two- and three-neutron forces at several resolution scales are presented and discussed in Sec. V. We end with a summary and conclusions.

II. QUASIPARTICLE INTERACTION IN NEUTRON MATTER

A. General structure of quasiparticle interaction and spin-space decomposition

In Landau's theory of normal Fermi liquids [24,25], the quasiparticle interaction $\mathcal{F}(\vec{p}_1 s_1 t_1;\, \vec{p}_2 s_2 t_2)$ derives from the change in the total energy density due to second-order variations in the particle occupation densities $\delta n_{\vec{p},s,t}$:

$$\delta\mathcal{E} = \sum_{\vec{p}st} \epsilon_{\vec{p}}\, \delta n_{\vec{p}st} + \frac{1}{2} \sum_{\substack{\vec{p}_1 s_1 t_1 \\ \vec{p}_2 s_2 t_2}} \mathcal{F}(\vec{p}_1 s_1 t_1;\, \vec{p}_2 s_2 t_2) \delta n_{\vec{p}_1 s_1 t_1}\, \delta n_{\vec{p}_2 s_2 t_2} + \cdots, \quad (1)$$

where s_i and t_i label the spin and isospin quantum numbers of the ith quasiparticle. The most general form for the effective interaction between two quasiparticles in pure neutron matter in the long-wavelength limit is given in Ref. [17]

$$\begin{aligned}\mathcal{F}(\vec{p}_1,\, \vec{p}_2) = {} & f(\vec{p}_1,\, \vec{p}_2) + g(\vec{p}_1,\, \vec{p}_2) \vec{\sigma}_1 \cdot \vec{\sigma}_2 \\ & + h(\vec{p}_1,\, \vec{p}_2) S_{12}(\hat{q}) + k(\vec{p}_1,\, \vec{p}_2) S_{12}(\hat{P}) \\ & + l(\vec{p}_1,\, \vec{p}_2) (\vec{\sigma}_1 \times \vec{\sigma}_2) \cdot (\hat{q} \times \hat{P}), \end{aligned} \quad (2)$$

where $\vec{q} = \vec{p}_1 - \vec{p}_2$ is the momentum transfer in the exchange channel, $\vec{P} = \vec{p}_1 + \vec{p}_2$ is the conserved center-of-mass momentum, and the tensor operator $S_{12}(\hat{v})$ is defined by $S_{12}(\hat{v}) = 3\vec{\sigma}_1 \cdot \hat{v} \vec{\sigma}_2 \cdot \hat{v} - \vec{\sigma}_1 \cdot \vec{\sigma}_2$. The interaction in Eq. (2) is invariant under parity and time-reversal transformations as well as under the interchange of the particle labels. However, due to the presence of the medium, Galilean invariance is no longer manifest, leading to new operator structures [namely, $S_{12}(\hat{P})$ and $A_{12}(\hat{q}, \hat{P}) = (\vec{\sigma}_1 \times \vec{\sigma}_2) \cdot (\hat{q} \times \hat{P})$] that depend explicitly on the center-of-mass momentum $\vec{P}$. Since the two quasiparticle momenta lie on the Fermi surface $|\vec{p}_1| = |\vec{p}_2| = k_f$, the remaining angular dependence of the quasiparticle interaction is conveniently expanded in Legendre polynomials of $\cos\theta = \hat{p}_1 \cdot \hat{p}_2$:

$$\chi(\vec{p}_1, \vec{p}_2) = \sum_{L=0}^{\infty} \chi_L(k_f) P_L(\cos\theta), \quad (3)$$

where χ represents f, g, h, k, or l, and the angle θ is related to the relative momentum $q = |\vec{p}_1 - \vec{p}_2|$ through the relation $q = 2k_f \sin(\theta/2)$.

The Fermi liquid parameters of nuclear matter can be either extracted from experiment (due to direct relations between particular Landau parameters and nuclear observables [25,26]) or computed microscopically within many-body perturbation theory [27]. Given a strongly interacting normal Fermi system at low temperatures, it is not clear that a perturbative approach is justified. However, in the case of nuclear and neutron matter, there are strong indications that renormalization group techniques [22,23,28] may render nuclear interactions perturbative for a wide range of densities when evolved down to a cutoff scale $\Lambda \lesssim 2.1$ fm^{-1}. In the framework of many-body perturbation theory, the quasiparticle interaction is extracted by functionally differentiating the contributions to the ground-state energy density twice with respect to the

particle occupation numbers. Previous work [1,2] has shown that a satisfactory description of bulk nuclear matter properties around the saturation density can be obtained with chiral and low-momentum nuclear interactions only with the inclusion of the leading-order Pauli-blocking and medium-polarization effects from two- and three-nucleon interactions. This requires a second-order perturbative calculation in the case of two-nucleon interactions together with the first-order perturbative contribution from three-nucleon forces. These systematic calculations suggest that a consistent microscopic description of the quasiparticle interaction in neutron matter, for which there is much less empirical information, can be achieved.

The relations between specific Fermi liquid parameters and bulk properties of the medium are well known [25,26]. The compression modulus of neutron matter [at density $\rho = k_f^3/(3\pi^2)$]

$$\mathcal{K} = \frac{3k_F^2}{M^*}(1+F_0) \tag{4}$$

is related to the Fermi liquid parameter $F_0 = N_0 f_0$ (with $N_0 = k_f M^*/\pi^2$ being the density of states at the Fermi surface) which represents the isotropic part of the spin-independent quasiparticle interaction. Note that the compressibility $\mathcal{K} = k_f^2 \partial^2 \bar{E}/\partial k_f^2 + 4k_f \partial \bar{E}/\partial k_f$ is determined by both the curvature and slope of the energy per particle $\bar{E}$. In Eq. (4) the quasiparticle effective mass M^* is given by

$$\frac{M^*}{M_n} = 1 + \frac{F_1}{3}, \tag{5}$$

with $M_n = 939.6$ MeV being the free neutron mass and $F_1 = N_0 f_1$. Considering only the central components of the quasiparticle interaction, the neutron matter spin susceptibility is given by

$$\chi = \mu_n^2 \frac{N_0}{1+G_0}, \tag{6}$$

where $\mu_n = -1.913$ is the free-space neutron magnetic moment (in units of the nuclear magneton) and $G_0 = N_0 g_0$. The presence of noncentral components in the quasiparticle interaction that couple quasiparticle spins to their momenta results in effective charges (magnetic moments) that are not scalars under rotations of the quasiparticle momentum. The resulting expression for the spin susceptibility then involves both longitudinal and transverse components of the magnetic moment [10,11].

A calculation to extract all components of the quasiparticle interaction given in Eq. (2) for an arbitrary two-neutron force was performed in Ref. [17]. In the following we present a general method to project out the various momentum-dependent scalar functions f, g, h, k, and l of the quasiparticle interaction in Eq. (2). This is achieved by taking specific linear combinations of the spin-space matrix elements of the quasiparticle interaction. The form of this matrix will of course depend on the choice of coordinate system. For $\vec{q} = \vec{p}_1 - \vec{p}_2 = q\vec{e}_z$ and $\vec{P} = \vec{p}_1 + \vec{p}_2 = P\vec{e}_x$, the spin-space matrix elements $\langle m_s|\mathcal{F}(\vec{p}_1, \vec{p}_2)|m_s'\rangle$ in terms of the scalar functions f, g, h, k, and l are given in Table I. The upper left 3×3 submatrix gives the nine triplet-triplet matrix elements, while the fourth row and fourth column give the matrix elements that include the singlet state. In this coordinate frame, the exchange tensor interaction $h(\vec{p}_1, \vec{p}_2)S_{12}(\hat{q})$ gives nonzero contributions only for the diagonal triplet spin-space matrix elements. The center-of-mass tensor force $k(\vec{p}_1, \vec{p}_2)S_{12}(\hat{P})$ contributes to the triplet diagonal matrix elements as well as the matrix elements mixing $m_s = \pm 1$ with $m_s' = \mp 1$. The cross-vector interaction $l(\vec{p}_1, \vec{p}_2)A_{12}(\hat{q}, \hat{P})$ is nonvanishing only in spin-nonconserving transitions with $|m_s - m_s'| = 1$. We note that it is not possible to separate the exchange tensor from the center-of-mass tensor interaction when considering only diagonal spin-space matrix elements, since they appear in the same linear combination $2h - k$. An alternative choice of coordinate system in which $\vec{q} = q\vec{e}_x$ and $\vec{P} = P\vec{e}_z$ just interchanges the contributions of the exchange tensor and center-of-mass tensor operators (and l comes with opposite sign).

TABLE I. Spin-space matrix elements $\langle m_s|\mathcal{F}(\vec{p}_1, \vec{p}_2)|m_s'\rangle$ in terms of scalar functions f, g, h, k, and l.

m_s/m_s'	1	0	−1	0
1	$f+g+2h-k$	0	$3k$	$\sqrt{2}l$
0	0	$f+g-4h+2k$	0	0
−1	$3k$	0	$f+g+2h-k$	$\sqrt{2}l$
0	$\sqrt{2}l$	0	$\sqrt{2}l$	$f-3g$

From the above matrix, the scalar functions multiplying the spin-dependent operators are extracted as the following linear combinations of the spin-space matrix elements:

$$\begin{aligned} f &= \left(2\mathcal{F}^t_{1,1} + \mathcal{F}^t_{0,0} + \mathcal{F}^s_{0,0}\right)/4, \\ g &= \left(2\mathcal{F}^t_{1,1} + \mathcal{F}^t_{0,0} - 3\mathcal{F}^s_{0,0}\right)/12, \\ h &= \left(\mathcal{F}^t_{1,1} + \mathcal{F}^t_{1,-1} - \mathcal{F}^t_{0,0}\right)/6, \\ k &= \left(\mathcal{F}^t_{1,-1}\right)/3, \\ l &= \left(\mathcal{F}^{ts}_{1,0}\right)/\sqrt{2}, \end{aligned} \tag{7}$$

where the superscripts s, t distinguish spin-singlet and spin-triplet states of two quasiparticles, and the two subscripts label m_s and m_s', respectively. Only the function $l(\vec{p}_1, \vec{p}_2)$ multiplying the cross-vector operator $A_{12}(\hat{q}, \hat{P})$ depends on a singlet-triplet mixing matrix element.

B. First-order contribution

With the relations given in Eq. (7) we need to compute only the quasiparticle interaction in different total spin states. The first-order perturbative contribution to the energy density is given by

$$\mathcal{E}^{(1)}_{2N} = \frac{1}{2}\sum_{12}\langle \vec{k}_1 s_1; \vec{k}_2 s_2|\bar{V}|\vec{k}_1 s_1; \vec{k}_2 s_2\rangle n_1 n_2, \tag{8}$$

where $\bar{V} = (1 - P_{12})V$ denotes the antisymmetrized two-body potential, $n_j = \theta(k_f - |\vec{k}_j|)$ is the usual zero-temperature Fermi distribution, and the summation includes both spin and momenta. The corresponding

contribution to the quasiparticle interaction reads

$$\mathcal{F}^{(1)}_{2N}(\vec{p}_1 s_1;\ \vec{p}_2 s_2) = \langle \vec{p}_1 s_1;\ \vec{p}_2 s_2|\bar{V}|\vec{p}_1 s_1;\ \vec{p}_2 s_2\rangle \equiv \langle 12|\bar{V}|12\rangle. \tag{9}$$

Setting the relative momentum $\vec{q} = \vec{p}_1 - \vec{p}_2$ along the $\vec{e}_z$ direction and projecting onto Legendre polynomials $P_L(\hat{p}_1 \cdot \hat{p}_2)$, the Fermi liquid parameters are obtained from Eq. (9) in terms of the matrix elements of V depending on $p = q/2$ in a partial-wave representation:

$$\mathcal{F}_L(k_f;\ Sm_s m_s') = 2(2L+1)\sum_{ll'J} i^{l-l'}[1+(-1)^{l+S}]\sqrt{(2l+1)(2l'+1)}\langle l0Sm_s|JM\rangle \times \langle l'0Sm_s'|JM\rangle \int_0^{k_f} dp\,\frac{p}{k_f^2}\langle plSJM|V|pl'SJM\rangle P_L\left(1-2p^2/k_f^2\right), \tag{10}$$

where we are following the normalization convention in Ref. [1]. The leading-order contribution is simply a kinematically restricted form of the free-space interaction, which contains no center-of-mass–dependent components. Therefore, the only nonzero contributions to the quasiparticle interaction are f, g, and h. This is further reflected in the partial wave decomposition through the obvious property $M = m_s = m_s'$ implied by the Clebsch-Gordan coefficients in Eq. (10).

C. Second-order contributions

The contribution to the energy density from the two-neutron force at second-order in many-body perturbation theory has the form

$$\mathcal{E}^{(2)}_{2N} = \frac{1}{4}\sum_{1234}\frac{|\langle 12|\bar{V}|34\rangle|^2 n_1 n_2(1-n_3)(1-n_4)}{\epsilon_1+\epsilon_2-\epsilon_3-\epsilon_4}, \tag{11}$$

where in a plane-wave basis $\epsilon_j = \vec{k}_j^2/(2M_n^{(*)})$ is the single-particle energy associated with the momentum $\vec{k}_j$. Functionally differentiating twice with respect to the quasiparticle distribution functions yields four different contributions to the quasiparticle interaction:

$$\begin{aligned}\mathcal{F}^{(2)}_{2N}(\vec{p}_1 s_1 t_1;\ \vec{p}_2 s_2 t_2) = {}& \frac{1}{2}\sum_{34}\frac{|\langle 12|\bar{V}|34\rangle|^2(1-n_3)(1-n_4)}{\epsilon_1+\epsilon_2-\epsilon_3-\epsilon_4} \\ & + \frac{1}{2}\sum_{34}\frac{|\langle 12|\bar{V}|34\rangle|^2 n_3 n_4}{\epsilon_3+\epsilon_4-\epsilon_1-\epsilon_2} \\ & - \sum_{34}\frac{|\langle 13|\bar{V}|24\rangle|^2 n_3(1-n_4)}{\epsilon_1+\epsilon_3-\epsilon_2-\epsilon_4} \\ & - \sum_{34}\frac{|\langle 13|\bar{V}|24\rangle|^2 n_4(1-n_3)}{\epsilon_1+\epsilon_4-\epsilon_2-\epsilon_3}.\end{aligned} \tag{12}$$

A graphical representation of these terms is given in Fig. 1. The first two terms in Eq. (12) are called the particle-particle (pp) and hole-hole (hh) contributions, which have a very similar structure. The particle-particle contribution is given by

$$\mathcal{F}^{pp}(\vec{p}_1\vec{p}_2;\ Sm_s S'm_s') = \frac{1}{2}\sum_{\bar{S}\bar{m}_s}\int\frac{d^3k_3}{(2\pi)^3}\frac{d^3k_4}{(2\pi)^3}\frac{\langle \vec{p}_1\vec{p}_2 Sm_s|\bar{V}|\vec{k}_3\vec{k}_4\bar{S}\bar{m}_s\rangle\langle\vec{k}_3\vec{k}_4\bar{S}\bar{m}_s|\bar{V}|\vec{p}_1\vec{p}_2 S'm_s'\rangle}{\epsilon_{p_1}+\epsilon_{p_2}-\epsilon_{k_3}-\epsilon_{k_4}} \times(1-n_3)(1-n_4)(2\pi)^3\delta(\vec{p}_1+\vec{p}_2-\vec{k}_3-\vec{k}_4), \tag{13}$$

where we allow for the possibility that $m_s \neq m_s'$. The hole-hole contribution is easily obtained from Eq. (13) by changing the sign of the energy denominator and replacing the two particle distribution functions $(1-n_3)(1-n_4)$ with hole distribution functions $n_3 n_4$. In computing the pp and hh diagrams, we found it more convenient to align the total momentum $\vec{P}$ along the $\vec{e}_z$ direction and the relative momentum $\vec{q}$ along the $\vec{e}_x$ direction. For this choice of coordinate system h and k are just interchanged in Table I. In a partial-wave basis, the particle-particle contribution in Eq. (13) reads

$$\begin{aligned}\mathcal{F}^{pp}_L(Sm_s m_s') = {}& \frac{2L+1}{4\pi^2 k_F^2}\sum_{\substack{l_1 l_2 l_3 l_4 m m' \\ \bar{m}\bar{m}_s JJ'M}}\int_0^{k_F} dpp\int_p^\infty dk k^2 N(l_1 m l_2\bar{m} l_3 m' l_4\bar{m})P_{l_1}^m(0)P_{l_3}^{m'}(0) \\ & \times\frac{M_n}{p^2-k^2}i^{l_2+l_3-l_1-l_4}\mathcal{C}^{JM}_{l_1 m S m_s}\mathcal{C}^{JM}_{l_2\bar{m}S\bar{m}_s}\mathcal{C}^{J'M}_{l_3 m' S m_s'}\mathcal{C}^{J'M}_{l_4\bar{m}S\bar{m}_s}\int_{\max\{-x_0,-1\}}^{\min\{x_0,1\}} dx\,P_{l_2}^{\bar{m}}(x)P_{l_4}^{\bar{m}}(x) \\ & \times\langle pl_1 SJM|\bar{V}|kl_2 SJM\rangle\langle kl_4 SJ'M|\bar{V}|pl_3 SJ'M\rangle P_L\left(1-2p^2/k_F^2\right),\end{aligned} \tag{14}$$

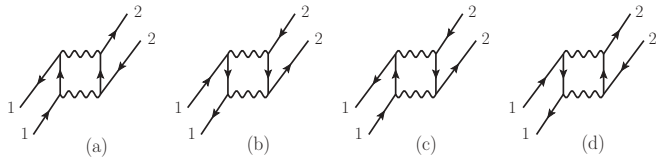

FIG. 1. Diagrams contributing to the second-order quasiparticle interaction (all interactions represented by wavy lines are antisymmetrized). Diagram (a) shows the particle-particle contribution, (b) shows the hole-hole contribution, and (c) and (d) show the particle-hole contributions.

where P_l^m are the associated Legendre functions, $x = \cos\theta_k$, $\vec{p} = (\vec{p}_1 - \vec{p}_2)/2$, $\vec{k} = (\vec{k}_3 - \vec{k}_4)/2$, $x_0 = (k^2 - p^2)/[2k(k_F^2 - p^2)^{1/2}]$ and $N(l_1 m l_2 \bar{m} l_3 m' l_4 \bar{m}) = N_{l_1}^m N_{l_2}^{\bar{m}} N_{l_3}^{m'} N_{l_4}^{\bar{m}}$ with $N_l^m = \sqrt{(2l+1)(l-m)!/(l+m)!}$. For $m_s = m_s'$, this expression agrees with Eq. (21) in Ref. [1]. From the underlying parity invariance of the two-neutron interaction, which preserves the total spin S, the pp and hh contributions cannot give rise to the spin-nonconserving cross-vector interaction. However, spin-orbit and tensor terms in the free-space neutron-neutron interaction do not conserve m_s and therefore can, at second-order in the pp and hh diagrams, give rise to a center-of-mass tensor interaction. This mechanism is exemplified in Sec. III with spin-orbit and tensor two-body model interactions.

We split the second-order particle-hole (ph) contribution into two pieces $\mathcal{F}_{ph}^{(c)} + \mathcal{F}_{ph}^{(d)}$ (see Fig. 1). The first term arises from a coupling of the incoming or outgoing quasiparticle 1 to a hole state, while for the second term quasiparticle 1 couples to a particle state. The explicit expression reads

$$\mathcal{F}_{ph}^{(c)}(\vec{p}_1\vec{p}_2; s_1s_2s_1's_2') = \sum_{s_3s_4}\int \frac{d^3k_3}{(2\pi)^3}\frac{d^3k_4}{(2\pi)^3}\frac{\langle \vec{p}_1\vec{k}_3 s_1s_3|\bar{V}|\vec{p}_2\vec{k}_4 s_2s_4\rangle\langle \vec{p}_2\vec{k}_4 s_2's_4|\bar{V}|\vec{p}_1\vec{k}_3 s_1's_3\rangle}{\epsilon_{p_2}+\epsilon_{k_4}-\epsilon_{p_1}-\epsilon_{k_3}} \times n_3(1-n_4)(2\pi)^3\delta(\vec{p}_1+\vec{k}_3-\vec{p}_2-\vec{k}_4), \tag{15}$$

where we allow for the possibility that the spin states of an incoming and outgoing quasiparticle can be different. In contrast to the treatment of the ph contribution to the central components of the quasiparticle interaction described in Ref. [1], here we have found it convenient to set $\vec{p}_1 - \vec{p}_2 = q\vec{e}_z$ and $\vec{p}_1 + \vec{p}_2 = P\vec{e}_x$. In this case we write

$$\begin{aligned}\mathcal{F}_L^{ph(c)}&(s_1s_2s_1's_2') \\ &= \frac{2L+1}{32\pi^3}\int_{-1}^{1} d\cos\theta\, P_L(\cos\theta)\int_0^{2\pi} d\phi_3\int_{\max\{0,y_0\}}^{k_f} dk_3k_3^2\int_{\max\{-1,z_0\}}^{1} d\cos\theta_3 \sum_{\substack{l_1l_2l_3l_4s_3s_4\\ m_1m_2m_3m_4}} \langle p' l_1 m_1 s_1 s_3|\bar{V}|k' l_2 m_2 s_2 s_4\rangle \\ &\times \langle k' l_4 m_4 s_2' s_4|\bar{V}|p' l_3 m_3 s_1' s_3\rangle \cos[(m_3 - m_1 + m_2 - m_4)\phi_{p'}] P_{l_1}^{m_1}(\cos\theta_{p'}) P_{l_2}^{m_2}(\cos\theta_{k'}) P_{l_3}^{m_3}(\cos\theta_{p'}) P_{l_4}^{m_4}(\cos\theta_{k'}) \\ &\times i^{l_2+l_3-l_1-l_4} N(l_1m_1l_2m_2l_3m_3l_4m_4)\frac{M_n}{k_fk_3\cos\theta_3\sin\frac{1}{2}\theta + k_f^2\sin^2\frac{1}{2}\theta},\end{aligned} \tag{16}$$

where $\vec{p}' = (\vec{p}_1 - \vec{k}_3)/2$, $\vec{k}' = (\vec{p}_2 - \vec{k}_4)/2$, $y_0 = k_f(1 - 2\sin\frac{1}{2}\theta)$, and $z_0 = (k_f^2 - k_3^2 - 4k_f^2\sin^2\frac{1}{2}\theta)/(4k_fk_3\sin\frac{1}{2}\theta)$. The product of exponentials coming from the spherical harmonics has been simplified to a cosine by noting that the imaginary part vanishes and that $\phi_{p'} = \phi_{k'}$. The expression in Eq. (16) can be further written out in terms of partial-wave matrix elements by first coupling to total spin S and then total angular momentum J. The extraction of the scalar functions f, g, h, k, and l is achieved by taking appropriate linear combinations of the sixteen spin-space matrix elements $\mathcal{F}_L(s_1s_2s_1's_2')$; namely,

$$\langle Sm_s|\mathcal{F}_L^{ph}|S'm_s'\rangle = \sum_{s_1s_1's_2s_2'} \mathcal{C}^{Sm_s}_{\frac{1}{2}s_1\frac{1}{2}s_2'}\mathcal{C}^{S'm_s'}_{\frac{1}{2}s_1'\frac{1}{2}s_2}\mathcal{F}_L^{ph}(s_1s_2s_1's_2'). \tag{17}$$

It is a good check of the calculation that the resulting spin-space matrix on the left-hand side of Eq. (17) is of the form introduced in Sec. II A.

The particle-hole polarization contribution can give rise to all noncentral interactions, as pointed out in Ref. [17]. However, the microscopic origin of the spin-nonconserving cross-vector interaction should be clarified. In fact, neither tensor forces nor spin-orbit forces alone, when iterated in the particle-hole channel, generate the cross-vector interaction. This can be seen from the spin structure of Eq. (15). In order to produce a nonvanishing singlet-triplet mixing matrix element, we can consider without loss of generality the spin-flip transition

$$\langle\uparrow\downarrow|\mathcal{F}_{ph}^{(c)}(\vec{p}_1\vec{p}_2)|\uparrow\uparrow\rangle \sim \sum_{s_3s_4}\langle\vec{p}_1\vec{k}_3\uparrow s_3|\bar{V}|\vec{p}_2\vec{k}_4\uparrow s_4\rangle \times \langle\vec{p}_2\vec{k}_4\downarrow s_4|\bar{V}|\vec{p}_1\vec{k}_3\uparrow s_3\rangle. \tag{18}$$

It is easily shown with momentum conservation ($\vec{p}_1 + \vec{k}_3 = \vec{p}_2 + \vec{k}_4$) that $\vec{p}' - \vec{k}' = \vec{p}_1 - \vec{p}_2 = q\vec{e}_z$. In this case, the free-space tensor force $\sim(3\sigma_1^z\sigma_2^z - \vec{\sigma}_1\cdot\vec{\sigma}_2)$ vanishes for $|\Delta m_s| = 1$, and therefore one of the two matrix elements in Eq. (18) will vanish for any values of s_3 and s_4. Similarly, for a free-space spin-orbit interaction of the form $iV_{so}(\vec{\sigma}_1 + \vec{\sigma}_2)\cdot(\vec{p}'\times\vec{k}')$, the vector $\vec{p}'\times\vec{k}'$ lies in the x-y plane and in this case the spin-orbit operator $(\vec{\sigma}_1 + \vec{\sigma}_2)\cdot(\vec{p}'\times\vec{k}')$ has very restricted matrix elements which are nonvanishing only in spin-triplet states with $|\Delta m_s| = 1$. Again, one of the matrix elements in Eq. (18) will vanish for any possible values of s_3 and s_4. These

arguments indicate that at second order only the interference of a spin-orbit interaction with any other (non-spin-orbit) component can produce the cross-vector interaction. In the following section, we will demonstrate that in fact central, spin-spin, and tensor components all give nonvanishing interference terms. Finally, we point out that although individually $\mathcal{F}_{ph}^{(c)}$ and $\mathcal{F}_{ph}^{(d)}$ can have forbidden matrix elements for $|\Delta m_s| = 1$ in the triplet states, when summed together such terms cancel exactly. All other spin-space matrix elements of $\mathcal{F}_{ph}^{(c)}$ and $\mathcal{F}_{ph}^{(d)}$ are identical. These features serve as a good check of the involved calculation of the quasiparticle interaction at second order.

D. Contribution from chiral three-neutron forces

Finally we consider the leading-order contribution from the N^{2}LO chiral three-nucleon force [20] in pure neutron matter. Only the components of the two-pion exchange three-nucleon force proportional to the low-energy constants c_1 and c_3 remain for neutrons:

$$V_{3n}^{(2\pi)} = \sum_{i\neq j\neq l} \frac{g_A^2}{4f_\pi^4} \frac{\vec{\sigma}_i\cdot\vec{q}_i\vec{\sigma}_j\cdot\vec{q}_j}{\left(\vec{q}_i^{\,2}+m_\pi^2\right)\left(\vec{q}_j^{\,2}+m_\pi^2\right)} \times\left(-2c_1m_\pi^2+c_3\vec{q}_i\cdot\vec{q}_j\right), \tag{19}$$

with parameters $g_A = 1.29$, $f_\pi = 92.4$ MeV and $m_\pi = 138$ MeV (average pion mass). The quantity $\vec{q}_i$ is the difference between the final and initial momenta of neutron i. In the following we employ two different choices for the low-energy constants c_1 and c_3 in Eq. (19). When combined with the bare chiral next-to next-to next-to leading order (N^{3}LO) nucleon-nucleon potential [19] we choose the values $c_1 = -0.81$ GeV^{-1} and $c_3 = -3.2$ GeV^{-1}, whereas with the low-momentum nucleon-nucleon potential $V_{\text{low-k}}$ we use $c_1 = -0.76$ GeV^{-1} and $c_3 = -4.78$ GeV^{-1} [29,30]. This variation in the low-energy constants (as well as the resolution scale Λ) provides a means for assessing theoretical uncertainty at a given order in many-body perturbation theory.

The first-order contribution to the energy density of neutron matter has the form

$$\mathcal{E}_{3n}^{(1)} = \frac{1}{6}\mathrm{Tr}_{\sigma_i,\sigma_j,\sigma_l}\int \frac{d^3k_i}{(2\pi)^3}\frac{d^3k_j}{(2\pi)^3}\frac{d^3k_l}{(2\pi)^3} n_i n_j n_l \langle ijl|\bar{V}_{3N}|ijl\rangle, \tag{20}$$

where $\bar{V}_{3n} = V_{3n}(1 - P_{12} - P_{23} - P_{13} + P_{12}P_{23} + P_{13}P_{23})$ is the fully antisymmetrized three-neutron interaction and $n_j = \theta(k_f - |\vec{k}_j|) + (2\pi)^3\delta^3(\vec{k}_j - \vec{p}_j)\delta n_{\vec{p}_j\sigma_j}$. Functionally differentiating twice with respect to the two quasiparticle distribution functions yields

$$\mathcal{F}_{3n}^{(1)}(\vec{p}_1,\ \vec{p}_2) = \frac{1}{2}\mathrm{Tr}_{\sigma_i}\int \frac{d^3k_i}{(2\pi)^3} n_i \langle i12|\bar{V}_{3n}|i12\rangle. \tag{21}$$

As we will see in Sec. IV, the form of the N^{2}LO chiral three-neutron force is sufficiently simple that in most cases analytical formulas for the Landau parameters are possible. We note that this leading-order contribution to the quasiparticle interaction from the N^{2}LO chiral three-neutron force is nearly equivalent to the effective interaction calculated previously in Refs. [31–33], although the quasiparticle interaction represents a restricted kinematical configuration for which the two interacting particles lie on the Fermi surface $|\vec{p}_{1,2}| = k_f$.

III. BENCHMARK CALCULATIONS WITH MODEL INTERACTIONS

In order to verify the spin-decomposition techniques and the accuracy of the intricate numerical calculations involved in the second-order calculation of the quasiparticle interaction, it is useful to examine simple model interactions that are amenable to (partial) analytical solutions. Intermediate-state momentum integrations and spin traces are carried out explicitly without decomposing the interaction into partial waves. For details on this approach to computing Fermi liquid parameters, see Ref. [18]. The diagrammatic contributions are shown in Fig. 2, where the double dash on a fermion line represents a "medium insertion." It is defined as the difference between the free-space propagator and the in-medium propagator:

$$i\left(\frac{\theta(|\vec{p}\,|-k_f)}{p_0-\vec{p}^{\,2}/(2M_n)+i\epsilon}+\frac{\theta(k_f-|\vec{p}\,|)}{p_0-\vec{p}^{\,2}/(2M_n)-i\epsilon}\right) = \frac{i}{p_0-\vec{p}^{\,2}/(2M_n)+i\epsilon} - 2\pi\delta(p_0-\vec{p}^{\,2}/(2M_n))\theta(k_f-|\vec{p}\,|). \tag{22}$$

Comparing with the expression given in Eq. (12), the sum of diagrams (a)–(d) corresponds to $\mathcal{F}_{pp}^{(2)} + \mathcal{F}_{hh}^{(2)}$. Expanding $(1-n_3)(1-n_4) = 1 - n_3 - n_4 + n_3n_4$ in the pp diagram, we see that the term proportional to n_3n_4 cancels the hole-hole contribution. Hence, the sum of the particle-particle and hole-hole diagrams gives just a free-space contribution and two terms with one medium insertion. The remaining diagrams (e)–(g) in Fig. 2 correspond to the particle-hole contribution in Eq. (12). In the following we consider only the Fermi liquid parameters $h_L(k_f)$, $k_L(k_f)$, and $l_L(k_f)$ associated with the noncentral components of the quasiparticle interaction.

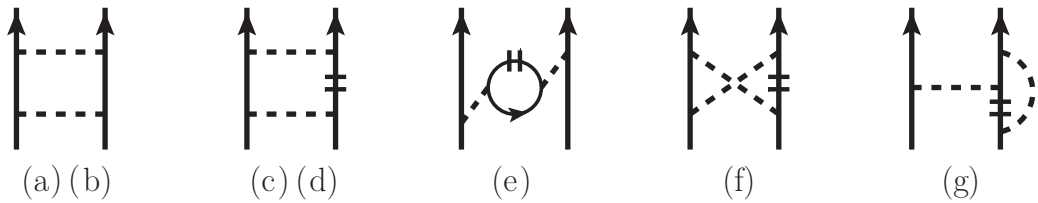

FIG. 2. Diagrammatic contributions to the second-order quasiparticle interaction in neutron matter. Diagrams (a)–(d) correspond to the sum of particle-particle and hole-hole contributions, while (e)–(g) together comprise the particle-hole contribution. Medium insertions are denoted by the short double lines, and the labels (b) and (d) refer to the crossed terms of (a) and (c). Reflected diagrams are not shown.

Detailed calculations for the central components have been presented in Ref. [1]. We provide explicit formulas for the relevant Landau parameters up to $L = 1$ obtained by first decomposing the effective interaction into the relevant operators and then projecting the expansion coefficients onto Legendre polynomials $P_L(\hat{p}_1 \cdot \hat{p}_2)$.

A. Pseudoscalar boson exchange to second order

We begin by considering pseudoscalar boson exchange with a "form factor" modification:

$$V(\vec{q}\,) = -\frac{g^2}{(m^2+q^2)^2}\vec{\sigma}_1 \cdot \vec{q}\vec{\sigma}_2 \cdot \vec{q}, \tag{23}$$

where g is a dimensionless coupling constant and m is the mass parameter chosen to be sufficiently large to achieve good convergence in momentum integrals and partial-wave summations. The momentum transfer is denoted by $\vec{q}$, and the squared denominator in Eq. (23) insures that all loop integrals converge. As discussed previously, the leading-order (free-space) contribution to the quasiparticle interaction contains only the exchange tensor interaction (in addition to the central components). Its $L = 0,\ 1$ projections are given by

$$h_0(k_f)^{(1)} = \frac{g^2}{3m^2}\left\{\frac{1}{4u^2}\ln(1+4u^2) - \frac{1}{1+4u^2}\right\}, \tag{24}$$

$$h_1(k_f)^{(1)} = \frac{g^2}{m^2}\left\{\frac{1+u^2}{4u^4}\ln(1+4u^2) - \frac{1}{u^2} + \frac{1}{1+4u^2}\right\}, \tag{25}$$

with the dimensionless parameter $u = k_f/m$. At second order, the direct contributions $\mathcal{F}^{(2a)}$ and $\mathcal{F}^{(2c)}$ have no noncentral components. The crossed term (b) of the iterated pseudoscalar-exchange diagram gives a contribution to the exchange tensor interaction:

$$h_0(k_f)^{(2b)} = \frac{g^4 M_n}{48\pi m^3}\left\{\frac{1}{2u^2}\ln\frac{1+2u^2}{1+u^2} - \frac{1}{1+2u^2} + \int_0^u dx \frac{1+4x^2+8x^4}{u^2(1+2x^2)^3}(\arctan 2x - \arctan x)\right\}, \tag{26}$$

$$h_1(k_f)^{(2b)} = \frac{g^4 M_n}{16\pi m^3}\left\{\frac{1}{1+2u^2} - \frac{1}{u^2} + \frac{2+u^2}{2u^4}\ln\frac{1+2u^2}{1+u^2} + \int_0^u dx \frac{u^2-2x^2}{u^4(1+2x^2)^3}(1+4x^2+8x^4) \times (\arctan 2x - \arctan x)\right\}. \tag{27}$$

Iterated pseudoscalar exchange does not include medium modifications and therefore cannot generate an effective interaction that depends explicitly on the center-of-mass momentum $\vec{P}$. In contrast, the crossed term (d) from the planar box diagram with Pauli blocking gives rise to an exchange tensor force and center-of-mass tensor force (as noted in Sec. II, the particle-particle and hole-hole diagrams cannot generate the cross-vector interaction). The associated $L = 0,\ 1$ exchange tensor Fermi liquid parameters are

$$h_0(k_f)^{(2d)} = \frac{g^4 M_n}{12\pi^2 k_f^3}\int_0^1 dx \int_{-1}^1 dy \int_{-1}^1 dz \frac{x^2}{[u^{-2}+A]^2[u^{-2}+B]^2}\left\{yz - x(x+y+z) - \frac{4x^2|y+z|}{A+B-4} + (1-x^2)^2\frac{(A+B)\eta\theta(W)}{(A+B-4)\sqrt{W}}\right\}, \tag{28}$$

$$h_1(k_f)^{(2d)} = \frac{g^4 M_n}{4\pi^2 k_f^3}\int_0^1 dx \int_{-1}^1 dy \int_{-1}^1 dz \frac{x^2}{[u^{-2}+A]^2[u^{-2}+B]^2}\left\{x^4 - x^2yz + x(y+z)(2-yz) + \frac{1}{2}(3y^2z^2 - y^2 - z^2 - 1) + \frac{4x^2|y+z|}{A+B-4} + x(1-x^2)^2(y+z-x)\frac{(A+B)\eta\theta(W)}{(A+B-4)\sqrt{W}}\right\}, \tag{29}$$

while the center-of-mass tensor Fermi liquid parameters are given by

$$k_0(k_f)^{(2d)} = \frac{g^4 M_n}{12\pi^2 k_f^3}\int_0^1 dx \int_{-1}^1 dy \int_{-1}^1 dz \frac{x^2}{[u^{-2}+A]^2[u^{-2}+B]^2}\left\{yz - x(3x+y+z) - \frac{8x^2|y+z|}{A+B-4} + \left[2x^2(2yz-1) + 3 + 3x^4 - 2x(1+x^2)(y+z) + \frac{8(1-x^2)^2}{A+B-4}\right]\frac{\eta\theta(W)}{\sqrt{W}}\right\}, \tag{30}$$

$$k_1(k_f)^{(2d)} = \frac{g^4 M_n}{4\pi^2 k_f^3}\int_0^1 dx \int_{-1}^1 dy \int_{-1}^1 dz \frac{x^2}{[u^{-2}+A]^2[u^{-2}+B]^2}\left\{3x^4 + x^2(2+yz) + x(y+z)(2-2x^2-yz) + \frac{1}{2}(3y^2z^2 - y^2 - z^2 - 1) + \frac{8x^2|y+z|}{A+B-4} + \left[x(y+z)(3+4x^2yz+5x^4) - 4 - 3x^6 - 2x^4(1+y^2+4yz+z^2) + x^2(5-2y^2-4yz-2z^2) - \frac{8(1-x^2)^2}{A+B-4}\right]\frac{\eta\theta(W)}{\sqrt{W}}\right\}, \tag{31}$$

with abbreviations: $A = 1 + x^2 - 2xy$, $B = 1 + x^2 - 2xz$, $W = (x-y)^2(x-z)^2 - (1-y^2)(1-z^2)$, and the sign $\eta = \mathrm{sgn}[(x-y)(x-z)]$. In fact, only the Pauli-blocked planar box diagram (d) gives rise to a center-of-mass tensor interaction from second-order pseudoscalar exchange.

Of the three diagrams (e)–(g) in Fig. 2 that encode the effects of medium polarization, (e) and (g) contribute to the quasiparticle interaction in the crossed channel and (f) contributes in the direct channel, regardless of the form of two-body interaction. In the case of pseudoscalar exchange only, (e) and (g) are nonvanishing for noncentral components. Diagram (e), representing the coupling of the boson to nucleon-hole states, yields for the exchange tensor interaction

$$h_0(k_f)^{(2e)} = \frac{8g^4M_n}{3\pi^2m^3u^2}\int_0^u dx\,\frac{x^4}{(1+4x^2)^4} \times\left[2ux + (u^2-x^2)\ln\frac{u+x}{u-x}\right], \quad (32)$$

$$h_1(k_f)^{(2e)} = \frac{8g^4M_n}{\pi^2m^3u^4}\int_0^u dx\,\frac{x^4(u^2-2x^2)}{(1+4x^2)^4} \times\left[2ux + (u^2-x^2)\ln\frac{u+x}{u-x}\right]. \quad (33)$$

The density-dependent vertex correction (g) can be split into a factorizable part

$$h_0(k_f)^{(2g)} = \frac{g^4M_n}{24\pi^2m^3u^3}\left[\frac{4u^2}{1+4u^2} - \ln(1+4u^2)\right] \times\left[\frac{1+2u^2}{4u^2}\ln(1+4u^2) - 1\right], \quad (34)$$

$$h_1(k_f)^{(2g)} = \frac{g^4M_n}{8\pi^2m^3u^5}\left[1 - \frac{1+2u^2}{4u^2}\ln(1+4u^2)\right] \times\left[(1+u^2)\ln(1+4u^2) - 3u^2 - \frac{u^2}{1+4u^2}\right], \quad (35)$$

and a nonfactorizable part

$$h_0(k_f)^{(2g')} = \frac{g^4M_n}{6\pi^2m^3u^2}\int_0^u dx\left[\ln(1+4x^2) - \frac{4x^2}{1+4x^2}\right] \times\left\{\frac{2ux(1+4u^2)^{-1}}{1+4u^2-4x^2} + \frac{u^2-x^2}{(1+4u^2-4x^2)^{3/2}} \times\ln\frac{(u\sqrt{1+4u^2-4x^2}+x)^2}{(1+4u^2)(u^2-x^2)}\right\}, \quad (36)$$

$$h_1(k_f)^{(2g')} = \frac{g^4M_n}{8\pi^2m^3u^4}\int_0^u dx\left[\ln(1+4x^2) - \frac{4x^2}{1+4x^2}\right] \times\left\{\frac{4ux(1+2u^2)}{(1+4u^2)(1+4u^2-4x^2)} - \ln\frac{u+x}{u-x} + \frac{1+(u^2-x^2)(6+4u^2)}{(1+4u^2-4x^2)^{3/2}} \times\ln\frac{(u\sqrt{1+4u^2-4x^2}+x)^2}{(1+4u^2)(u^2-x^2)}\right\}. \quad (37)$$

We note that diagrams (e)–(g), representing the particle-hole contribution, do not give rise to a cross-vector interaction in agreement with the general argument presented in Sec. II. We now evaluate the expressions given in Eqs. (26)–(37) choosing $g = 5$, $m = 300$ MeV, and $k_f = 1.7$ fm^{-1}. In Table II we compare these semi-analytical results to those obtained from a numerical evaluation of the second-order contributions as given in Sec. II through a partial-wave decomposition. The agreement is generally on the order of 2% or better.

TABLE II. The $L = 0$, 1 noncentral Fermi liquid parameters from the pseudoscalar exchange interaction in Eq. (23) at second order. We compare the sum of the particle-particle, hole-hole, and particle-hole diagrams computed numerically to the semi-analytical results of Eqs. (26)–(37).

Modified pseudoscalar boson exchange ($k_f = 1.7$ fm^{-1})				
	h_0 [fm^2]	k_0 [fm^2]	h_1 [fm^2]	k_1 [fm^2]
2nd (pp)	0.119	−0.147	−0.143	0.057
2nd (hh)	0.027	−0.062	−0.057	0.074
2nd (ph)	1.394	−0.001	0.913	−0.001
Total	1.540	−0.210	0.713	0.129
Analytical	1.552	−0.209	0.719	0.126

B. Spin-orbit interaction to second order

We consider as well the case of a pure spin-orbit interaction of the form

$$V_{so} = \frac{2g_s^2}{\left(m_s^2+q^2\right)^2} i(\vec{\sigma}_1+\vec{\sigma}_2)\cdot(\vec{q}\times\vec{p}\,), \quad (38)$$

where $\vec{q}$ is the momentum transfer, $\vec{p}$ is half the incoming relative momentum, and m_s is the mass of the exchanged boson to be fixed later. We consider only the isotropic ($L = 0$) contributions to the noncentral interactions. The first-order contribution from V_{so} to the quasiparticle interaction vanishes trivially since $\vec{q}\times\vec{p} = 0$. The direct term (a) of the planar box diagram gives the contribution

$$h_0(k_f)^{(2a)} = \frac{g_s^4M_n}{288\pi m_s^3}\left\{\frac{5+12u^2}{1+4u^2} - \frac{5}{4u^2}\ln(1+4u^2)\right\}, \quad (39)$$

with $u = k_f/m_s$, while the crossed-term (b) contribution reads

$$h_0(k_f)^{(2b)} = \frac{g_s^4M_n}{24\pi m_s^3}\left\{\frac{1}{2u^2}\ln\frac{1+2u^2}{1+u^2} - \frac{1}{1+2u^2} + \int_0^u dx\,\frac{1+4x^2+8x^4}{u^2(1+2x^2)^3}(\arctan 2x - \arctan x)\right\}. \quad (40)$$

For the Pauli-blocked planar box diagram, we find that the direct term (c) gives rise to both exchange tensor as well as center-of-mass tensor contributions of the form

$$h_0(k_f)^{(2c)} = \frac{g_s^4M_n}{6\pi^2k_f^3}\int_0^1 dx\int_{-1}^1 dy\int_{-1}^1 dz\,\frac{x^2}{[u^{-2}+A]^4} \times\left\{-x(x+y) - \frac{4x^2|y+z|}{A+B-4} + (1-x^2)^2\frac{(A+B)\eta\theta(W)}{(A+B-4)\sqrt{W}}\right\}, \quad (41)$$

$$k_0(k_f)^{(2c)} = \frac{g_s^4 M_n}{6\pi^2 k_f^3}\int_0^1 dx\int_{-1}^1 dy\int_{-1}^1 dz\frac{x^2}{[u^{-2}+A]^4} \times\left\{-x(3x+y)-\frac{8x^2|y+z|}{A+B-4} +\left[3+3x^4+2x^2(2yz-1)-2x(1+x^2) \times(y+z)+\frac{8(1-x^2)^2}{A+B-4}\right]\frac{\eta\theta(W)}{\sqrt{W}}\right\}, \quad (42)$$

with abbreviations: $A = 1+x^2-2xy$, $B = 1+x^2-2xz$, $W = (x-y)^2(x-z)^2-(1-y^2)(1-z^2)$ and $\eta = \mathrm{sgn}[(x-y)(x-z)]$. Likewise, the crossed term (d) of the Pauli-blocked planar box diagram yields

$$h_0(k_f)^{(2d)} = \frac{g_s^4 M_n}{6\pi^2 k_f^3}\int_0^1 dx\int_{-1}^1 dy\int_{-1}^1 dz \times\frac{x^2}{[u^{-2}+A]^2[u^{-2}+B]^2}\left\{yz-x(x+y+z) -\frac{4x^2|y+z|}{A+B-4}+(1-x^2)^2\frac{(A+B)\eta\theta(W)}{(A+B-4)\sqrt{W}}\right\}, \quad (43)$$

$$k_0(k_f)^{(2d)} = \frac{g_s^4 M_n}{6\pi^2 k_f^3}\int_0^1 dx\int_{-1}^1 dy\int_{-1}^1 dz \times\frac{x^2}{[u^{-2}+A]^2[u^{-2}+B]^2} \times\left\{yz-x(3x+y+z)-\frac{8x^2|y+z|}{A+B-4} +\left[2x^2(2yz-1)+3+3x^4-2x(1+x^2) \times(y+z)+\frac{8(1-x^2)^2}{A+B-4}\right]\frac{\eta\theta(W)}{\sqrt{W}}\right\}. \quad (44)$$

The coupling to intermediate particle-hole states (e) in the crossed channel generates both exchange and center-of-mass tensor interactions:

$$h_0(k_f)^{(2e)} = \frac{g_s^4 M_n}{(3\pi u)^2 m_s^3}\int_0^u dx\frac{x^2}{(1+4x^2)^4}\left[ux(15x^2-17u^2) -\frac{15}{2}(u^2-x^2)^2\ln\frac{u+x}{u-x}\right], \quad (45)$$

$$k_0(k_f)^{(2e)} = \frac{2g_s^4 M_n}{3\pi^2 u^2 m_s^3}\int_0^u dx\frac{x^2(x^2-u^2)}{(1+4x^2)^4} \times\left[2ux+(u^2-x^2)\ln\frac{u+x}{u-x}\right], \quad (46)$$

and for the Pauli-blocked crossed box diagram (f), the direct term produces the contributions

$$h_0(k_f)^{(2f)} = \frac{8g_s^4 M_n}{(3\pi u)^2 m_s^3}\int_0^u dx\frac{x^3}{(1+4x^2)^4}\left[u(u^2-x^2) +2u^3\ln\frac{u^2-x^2}{4u^2}-6ux^2\ln\frac{u^2-x^2}{4x^2} -4x^3\ln\frac{u+x}{u-x}\right], \quad (47)$$

$$k_0(k_f)^{(2f)} = \frac{8g_s^4 M_n}{3\pi^2 u^2 m_s^3}\int_0^u dx\frac{x^3}{(1+4x^2)^4}\left[u(u^2-x^2) -4ux^2\ln\frac{u^2-x^2}{4x^2}-2x(u^2+x^2)\ln\frac{u+x}{u-x}\right]. \quad (48)$$

Finally, the crossed term of the vertex correction diagram (g) reads

$$h_0(k_f)^{(2g)} = \frac{64g_s^4 M_n}{3\pi^2 k_f^3}\int_0^u dx\int_0^u dy\frac{x^3y^2}{(1+4x^2)^2(1+4y^2)^2} \times\left\{u\,\mathrm{Re}\ln\frac{x+\sqrt{x^2+y^2-u^2}}{u+y}+\frac{y}{u^2}(u^2-x^2) +\frac{x}{u^2-y^2}[u\,\mathrm{Re}\sqrt{x^2+y^2-u^2}-xy]\right\}, \quad (49)$$

$$k_0(k_f)^{(2g)} = \frac{64g_s^4 M_n}{3\pi^2 k_f^3}\int_0^u dx\int_0^u dy\frac{x^3y^2}{(1+4x^2)^2(1+4y^2)^2} \times\left\{\frac{y}{u^2}(u^2-x^2)+\frac{2x}{u^2-y^2} \times[u\,\mathrm{Re}\sqrt{x^2+y^2-u^2}-xy]\right\}, \quad (50)$$

where Re stands for real part. Again, we find that the spin-orbit interaction iterated to second order does not give rise to a cross-vector interaction. We choose the parameters $g_s = 10$, $m_s = 700$ MeV, and $k_f = 1.7$ fm^{-1}. In Table III we compare the sum of the particle-particle and hole-hole diagrams to the sum of diagrams (a)–(d) in Fig. 2. Likewise, we compare the particle-hole contribution to the sum of diagrams (e)–(g) in Fig. 2. The results of both calculations are again in very good numerical agreement with one another. We note that the similarity among several Fermi liquid parameters; namely, $h_0^{pp+hh} \simeq -h_0^{ph} \simeq -k_0^{pp+hh+ph}$, is merely a coincidence resulting from our choice of scalar particle mass.

TABLE III. The $L = 0$ noncentral Fermi liquid parameters for the spin-orbit interaction at second order. The numerical results for h_0 and k_0 based on the partial-wave decomposition are compared with values from the semi-analytical formulas in Eqs. (39)–(50).

Spin-orbit interaction ($k_f = 1.7$ fm^{-1})		
	h_0 [fm^2]	k_0 [fm^2]
2nd ($pp+hh$)	0.761	−0.311
2nd (ph)	−0.758	−0.444
Total	0.003	−0.756
Analytical ($pp+hh$)	0.772	−0.312
Analytical (ph)	−0.761	−0.448
Total	0.011	−0.760

C. Spin-nonconserving cross-vector interaction

As mentioned in Sec. II C, the origin of the spin-nonconserving quasiparticle interaction [proportional to the cross-vector operator $(\sigma_1 \times \sigma_2) \cdot (\hat{q} \times \hat{P})$] is the interference of the spin-orbit component of the two-body potential with its other (central, spin-spin, and tensor) components. In order to exemplify this mechanism through a solvable model, we consider a simple contact interaction with couplings in all relevant channels:

$$V_{\rm ct} = \Gamma_c + \Gamma_s \vec{\sigma}_1 \cdot \vec{\sigma}_2 + \Gamma_t \vec{\sigma}_1 \cdot \vec{q} \vec{\sigma}_2 \cdot \vec{q} + i\Gamma_{so} (\vec{\sigma}_1 + \vec{\sigma}_2) \cdot (\vec{q} \times \vec{p}) \,. \tag{51}$$

At second order the interference terms arising from the particle-hole diagrams (e)–(g) in Fig. 2 can be worked out analytically. One finds for the first three Landau parameters of the cross-vector interaction

$$l_0 = \frac{M_n k_f^3}{5\pi}(\Gamma_c - 3\Gamma_s)\Gamma_{so}, \quad l_1 = \frac{3M_n k_f^3}{70\pi}(\Gamma_c - 3\Gamma_s)\Gamma_{so}, \quad l_2 = \frac{11 M_n k_f^3}{84\pi}(3\Gamma_s - \Gamma_c)\Gamma_{so}, \tag{52}$$

$$l_0 = -\frac{8M_n k_f^5}{21\pi}\Gamma_t \Gamma_{so}, \quad l_1 = -\frac{4M_n k_f^5}{21\pi}\Gamma_t \Gamma_{so}, \quad l_2 = \frac{50 M_n k_f^5}{231\pi}\Gamma_t \Gamma_{so}. \tag{53}$$

Due to their different structure we have listed separately the interference terms with central and spin-spin interactions and the "tensor-type" interaction $\Gamma_t \vec{\sigma}_1 \cdot \vec{q}\, \vec{\sigma}_2 \cdot \vec{q}$. Our second-order calculation based on a decomposition of the two-body potential into partial-wave matrix elements reproduced these analytical results with good numerical accuracy. In the absence of the tensor term, the condition $\Gamma_c = 3\Gamma_s$ (giving $l_L = 0$) is equivalent to a vanishing interaction in the spin-singlet state.

IV. LANDAU PARAMETERS FROM CHIRAL 3N INTERACTION

In this section we consider the N^{2}LO chiral three-nucleon force in neutron matter and derive expressions for all $L = 0,\ 1$ Landau parameters arising from the leading-order (one-loop) contribution to the quasiparticle interaction. In most cases it is possible to obtain analytical expressions for arbitrary values of L, but for brevity we show only the formulas for the isotropic ($L = 0$) and p-wave ($L = 1$) parameters. As mentioned in Sec. II D, we keep only the two-pion exchange three-neutron force proportional to c_1 and c_3. There are three one-loop diagrams contributing to the effective interaction, shown in Fig. 3, which we label as $V_{NN}^{{\rm med},i}$ for $i = 1,\ 2,\ 3$. Both the pion self-energy correction $V_{NN}^{\rm med,1}$ and the vertex correction $V_{NN}^{\rm med,2}$ produce an effective interaction similar to that of one-pion exchange. Both terms vanish in the direct channel but give contributions to f, g, and h in the exchange channel. For the pion self-energy correction we find

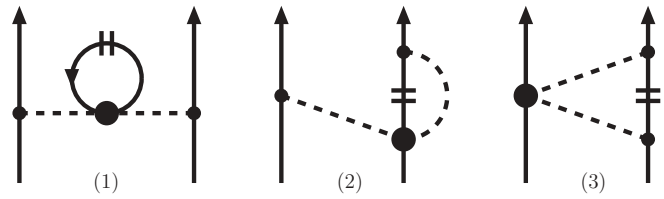

FIG. 3. Diagrammatic contributions to the quasiparticle interaction in neutron matter generated from the two-pion exchange three-neutron interaction. The short double-line symbolizes summation over the filled Fermi sea of neutrons. Reflected diagrams of (2) and (3) are not shown.

$$\mathcal{F}_0(k_f)^{(\rm med,1)} f = [3 - \vec{\sigma}_1 \cdot \vec{\sigma}_2 + 2S_{12}(\hat{q})]\frac{g_A^2 m_\pi^3}{(6\pi)^2 f_\pi^4} \times \left\{ \frac{(2c_1 - c_3)u^3}{1+4u^2} - c_3 u^3 + (c_3 - c_1)\frac{u}{2}\ln(1+4u^2) \right\}, \tag{54}$$

$$\mathcal{F}_1(k_f)^{(\rm med,1)} = [3 - \vec{\sigma}_1 \cdot \vec{\sigma}_2 + 2S_{12}(\hat{q})]\frac{g_A^2 m_\pi^3}{48\pi^2 f_\pi^4} \times \left\{ \frac{(2c_1 - c_3)u}{1+4u^2} + (6c_1 - 5c_3)u + \left[2(c_3 - c_1)u + \frac{3c_3 - 4c_1}{2u} \right] \times \ln(1+4u^2) \right\}, \tag{55}$$

with $u = k_f/m_\pi$. As seen from the above formulas, the expressions for the Fermi liquid parameters of the central, spin-spin, and tensor quasiparticle interaction are identical up to integer factors characteristic of a one-pion exchange nucleon-nucleon potential. The contribution from the crossed term of the pion exchange vertex correction $V_{NN}^{\rm med,2}$ reads

$$\mathcal{F}_0(k_f)^{(\rm med,2)} = [3 - \vec{\sigma}_1 \cdot \vec{\sigma}_2 + 2S_{12}(\hat{q})]\frac{g_A^2 m_\pi^3}{(24\pi)^2 f_\pi^4} \left\{ \frac{3c_1}{4u^5}[8u^4 + 4u^2 - (1+4u^2)\ln(1+4u^2)][4u^2 - \ln(1+4u^2)] + c_3 \left[\frac{4}{u^2}(4u^2 - \ln(1+4u^2))\arctan 2u + \frac{48u^4 + 16u^2 + 3}{32u^7}\ln^2(1+4u^2) + \frac{40u^3}{3} - 22u + \frac{2}{u} + \frac{3}{2u^3} + \frac{12u^4 - 16u^6 - 30u^2 - 9}{12u^5}\ln(1+4u^2) \right] \right\}, \tag{56}$$

$$\mathcal{F}_1(k_f)^{(\mathrm{med},2)} = [3-\vec{\sigma}_1\cdot\vec{\sigma}_2+2S_{12}(\hat{q})]\frac{g_A^2 m_\pi^3}{(16\pi)^2 f_\pi^4}\left\{\frac{c_1}{2u^7}[4u^2-(1+2u^2)\ln(1+4u^2)][8u^4+4u^2-(1+4u^2)\ln(1+4u^2)]\right.$$
$$+\frac{c_3}{3u^4}\left[8(4u^2-(1+2u^2)\ln(1+4u^2))\arctan 2u+\frac{96u^6+80u^4+22u^2+3}{16u^5}\ln^2(1+4u^2)\right.$$
$$\left.\left.+\frac{56u^6-32u^8-60u^4-48u^2-9}{6u^3}\ln(1+4u^2)+\frac{8u^5}{3}(7-4u^2)-28u^3+10u+\frac{3}{u}\right]\right\}. \quad (57)$$

Lastly, we compute the $L=0,\,1$ Landau parameters associated with the Pauli-blocked two-pion exchange diagram $V_{NN}^{\mathrm{med},3}$, which has a more complicated spin structure than $V_{NN}^{\mathrm{med},1}$ and $V_{NN}^{\mathrm{med},2}$. Both the direct and exchange terms contribute, and the central components of the quasiparticle interaction read

$$\mathcal{F}_0(k_f)^{(\mathrm{med},3)} = \frac{g_A^2 m_\pi^3}{16\pi^2 f_\pi^4}\left\{8(c_3-c_1)u-\frac{8c_3u^3}{3}\right.$$
$$+\frac{3c_3-4c_1}{u}\ln(1+4u^2)$$
$$+(12c_1-10c_3)\arctan 2u+(1+\vec{\sigma}_1\cdot\vec{\sigma}_2)$$
$$\left.\times\int_0^u dx\left[2c_1Z^2+\frac{c_3}{3}(X^2+2Y^2)\right]\right\}, \quad (58)$$

$$\mathcal{F}_1(k_f)^{(\mathrm{med},3)} = (1+\vec{\sigma}_1\cdot\vec{\sigma}_2)\frac{g_A^2 m_\pi^3}{16\pi^2 f_\pi^4}\int_0^u dx\left\{2c_1\left(Z_a^2+2Z_b^2\right)\right.$$
$$\left.+c_3\left(X_a^2+2X_b^2+\frac{4}{3}X_c^2\right)\right\}. \quad (59)$$

The auxiliary functions $X,\ Y,\ Z;\ X_a,\ X_b,\ X_c$; and $Z_a,\ Z_b$ are defined in Sec. 2.2 of Ref. [2]. Concerning the noncentral quasiparticle interaction, $V_{NN}^{\mathrm{med},3}$ produces no tensor forces in pure neutron matter. However, one expects $V_{NN}^{\mathrm{med},3}$ to generate an exchange tensor force in symmetric nuclear matter [32] since in this case the three-nucleon force proportional to c_4 does not vanish. As a special feature, the crossed term of the Pauli-blocked 2π exchange diagram gives rise to a cross-vector interaction. With its usual representation given by

$$\mathcal{F}_{\mathrm{cross}} = (\vec{\sigma}_1\times\vec{\sigma}_2)\cdot(\hat{q}\times\hat{P})\sum_{L=0}^{\infty} l_L(k_f)P_L(\hat{p}_1\cdot\hat{p}_2), \quad (60)$$

a complete analytical solution for the Landau parameters $l_L(k_f)$ could not be obtained. When choosing the alternative form of the cross-vector interaction

$$\mathcal{F}_{\mathrm{cross}} = \frac{(\vec{\sigma}_1\times\vec{\sigma}_2)\cdot(\vec{p}_1\times\vec{p}_2)}{|\vec{p}_1+\vec{p}_2|^2}\sum_{L=0}^{\infty}\tilde{l}_L(k_f)P_L(\hat{p}_1\cdot\hat{p}_2), \quad (61)$$

all occurring integrals can be solved analytically in the present case. The results for the Landau parameters read

$$\tilde{l}_0(k_f)^{(\mathrm{med},3)} = \frac{g_A^2 m_\pi^3}{(8\pi)^2 f_\pi^4}\left\{\frac{c_1}{u^3}[16u^4-(1+4u^2)\ln^2(1+4u^2)]\right.$$
$$\left.+c_3\left[4u^3-8u-\frac{1}{u}+\frac{1+4u^2}{2u^3}\ln(1+4u^2)+\left(\frac{1}{u}-\frac{1}{16u^5}\right)\ln^2(1+4u^2)\right]\right\}, \quad (62)$$

$$\tilde{l}_1(k_f)^{(\mathrm{med},3)} = \frac{g_A^2 m_\pi^3}{(8\pi)^2 f_\pi^4}\left\{3c_1\left[8u-\frac{8}{u}-\frac{2}{u^3}+\frac{8u^4+6u^2+1}{u^5}\ln(1+4u^2)-\frac{32u^6+24u^4+8u^2+1}{8u^7}\ln^2(1+4u^2)\right]\right.$$
$$+c_3\left[\frac{20u^3}{3}-16u-\frac{2}{u}-\frac{3}{u^3}-\frac{3}{4u^5}+\frac{16u^6+28u^4+18u^2+3}{8u^7}\right.$$
$$\left.\left.\times\ln(1+4u^2)+\frac{3}{64u^9}(64u^8-20u^4-8u^2-1)\ln^2(1+4u^2)\right]\right\}. \quad (63)$$

The exact relation between these two representations of the cross-vector interaction is given by

$$l_L = \sum_{L'=0}^{\infty} a_{LL'}\tilde{l}_{L'}, \quad (64)$$

with coefficients $a_{LL'} = \frac{1}{4}(2L+1)\int_{-1}^{1} dz\sqrt{(1-z)/(1+z)}\,P_L(z)P_{L'}(z)$, which are all nonvanishing rational multiples of π. However, since infinitely many terms are involved, this (exact) relation is of limited practical use. The numerical results assuming the standard form in Eq. (60) of the cross-vector interaction will be shown in the following section.

V. RESULTS

A. Neutron matter equation of state

The Fermi liquid parameters in neutron matter, unlike those in symmetric nuclear matter close to the saturation density, are largely unconstrained by empirical data. Given

that our perturbative treatment of the quasiparticle interaction includes only the leading-order medium corrections from two- and three-body forces, it is useful to compare the associated zero-temperature equation of state of neutron matter (at the same order in perturbation theory) with those obtained using nonperturbative methods. As a benchmark we consider variational calculations [34] of neutron matter employing the high-precision Argonne v_{18} two-nucleon potential [35] together with the Urbana UIX three-body potential [36], which provide a realistic description of light nuclei and nuclear matter.

In the partial-wave representation of the two-body interaction, the first-order contribution to the energy per particle $\bar{E} = E/A$ reads

$$\bar{E}^{(1)}_{2n}(k_f) = \frac{1}{2\pi^2 k_f^3}\sum_{lSJ}(2J+1)\int_0^{k_f} dp p^2 (k_f - p)^2 \times (2k_f + p)\langle plSJ|\bar{V}|plSJ\rangle, \tag{65}$$

and the more intricate second-order contribution takes the form

$$\bar{E}^{(2)}_{2n}(k_f) = \frac{6}{(4\pi)^4 k_f^3}\sum_{\substack{l_1 l_2 l_3 l_4 \\ S m_s m_s' J J' M}}\int_0^{2k_f} dp' p'^2 \int_0^{\sqrt{k_f^2 - p'^2/4}} dp p^2 \int_{\sqrt{k_f^2 - p'^2/4}}^{\infty} dq q^2 N(l_1 m l_2 m' l_3 m l_4 m') \times i^{l_2 + l_3 - l_1 - l_4}\frac{M_n}{p^2 - q^2}\mathcal{C}^{JM}_{l_1 m S m_s}\mathcal{C}^{JM}_{l_2 m' S m_s'}\mathcal{C}^{J'M}_{l_3 m S m_s}\mathcal{C}^{J'M}_{l_4 m' S m_s'}\langle pl_1 SJ|\bar{V}|ql_2 SJ\rangle\langle ql_4 SJ'|\bar{V}|pl_3 SJ'\rangle \times \int_{-x_p}^{x_p} d\cos\theta_p P^m_{l_1}(\cos\theta_p)P^m_{l_3}(\cos\theta_p)\int_{-x_q}^{x_q} d\cos\theta_q P^{m'}_{l_2}(\cos\theta_q)P^{m'}_{l_4}(\cos\theta_q), \tag{66}$$

where $x_p = \min\{1, (k_f^2 - p^2 - p'^2/4)/(pp')\}$ and $x_q = \min\{1, (q^2 - k_f^2 + p'^2/4)/(qp')\}$. In Appendix A we provide the analytical expressions for the second-order contributions to the energy per particle associated with the two model interactions introduced in Sec. III. Finally, the leading-order chiral three-neutron interaction leads to Hartree and Fock contributions to the energy per particle of neutron matter of the combined form

$$\bar{E}^{(1)}_{3n}(k_f) = \frac{g_A^2 m_\pi^6}{(2\pi f_\pi)^4}\left\{(6c_1 - 5c_3)\frac{u^3}{3}\arctan 2u - \frac{2c_3}{9}u^6 + (c_3 - c_1)u^4 + (3c_1 - 2c_3)\frac{u^2}{6} + \left[\frac{c_3}{12} - \frac{c_1}{8} + \frac{u^2}{4}(3c_3 - 4c_1)\right] \times \ln(1 + 4u^2) + \frac{1}{32u^3}\int_0^u dx\left[6c_1 H^2 + c_3\left(G_S^2 + 2G_T^2\right)\right]\right\}, \tag{67}$$

with $u = k_f/m_\pi$. The auxiliary functions H, G_S, and G_T are defined in Eqs. (24)–(26) of Ref. [37]. These interaction contributions are added to the relativistically improved kinetic energy per particle $\bar{E}_{\rm kin}(k_f) = 3k_f^2/(10M_n) - 3k_f^4/(56M_n^3)$.

In Fig. 4 we plot the resulting equation of state of neutron matter for densities up to $\rho \simeq 1.5\rho_0$. For both chiral and low-momentum interactions one finds good agreement with the results of the variational calculation of Ref. [34], labeled "APR" in the figure. The difference between the two perturbative calculations arises primarily from the different values of low-energy constants c_1 and c_3. Note that the recent neutron matter calculation [38] including the subleading chiral three- and four-neutron interactions gives very similar results. For comparison, we have included in Fig. 4 the result for the neutron matter equation of state obtained in a recent quantum Monte Carlo (QMC) simulation [39] employing phenomenological density-dependent two-body potentials. The data points for the lowest two densities are taken from a different quantum Monte Carlo calculation in Ref. [40]. For later comparison, we compute the compressibility of neutron matter directly from the energy per particle. We find that at $\rho = 0.166$ fm^{-1}, $\mathcal{K} = 560$ and 650 MeV for the unevolved chiral interaction and low-momentum potential $V_{\text{low-k}}$, respectively.

B. Neutron matter quasiparticle interaction

In this section we present and discuss the calculations of the $L = 0$, 1, 2 Landau parameters for the quasiparticle interaction in neutron matter from chiral and low-momentum two- and three-nucleon forces. We begin by considering the leading-order (free-space) contribution from both the bare chiral N^{3}LO NN interaction [19] as well as the low-momentum NN potential $V_{\text{low-k}}$ [22,23] obtained by integrating out momenta beyond the cutoff scale of 2.1 fm^{-1}. We use the general formula in Eq. (9) for computing the first-order perturbative contribution to the quasiparticle interaction as well as the projection formulas in Eq. (7) for extracting the scalar functions f, g, and h. In Table IV we show the results for neutron matter with a Fermi momentum of $k_f = 1.7$ fm^{-1} corresponding to a density of $\rho_0 = 0.166$ fm^{-3}. In both cases the Fermi liquid parameters decrease rapidly in magnitude with L for all channels. For larger values of L the difference between bare and evolved two-neutron interactions is strongly reduced, and at $L = 3$ it is almost negligible. Short-distance repulsion in the bare chiral NN interaction is integrated out through the renormalization-group evolution, leading to a significant reduction in f_0. For both potentials, the compressibility $\mathcal{K}$ of neutron matter at ρ_0 would be unphysically small. This feature is shared by many leading-order perturbative calculations

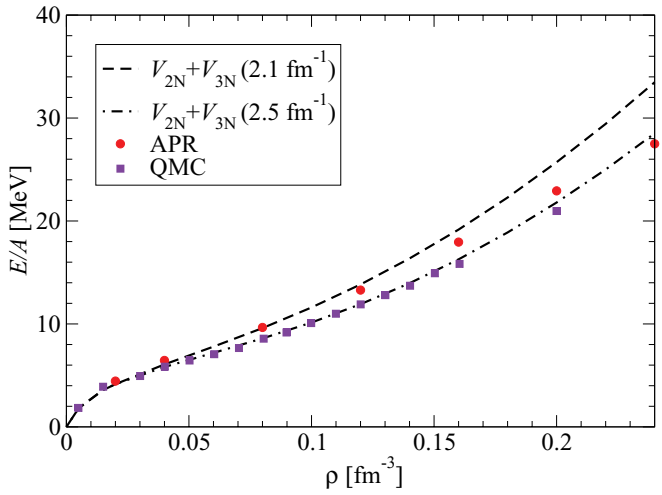

FIG. 4. (Color online) Energy per particle of neutron matter from chiral and low-momentum two- and three-body interactions. The cutoff scale associated with the bare chiral nuclear potential is $\Lambda = 2.5$ fm^{-1}, while that of the low-momentum interaction is $\Lambda = 2.1$ fm^{-1}. The curve labeled "APR" is taken from the variational calculations of Akmal *et al.* [34], and the curve labeled "QMC" is taken from the quantum Monte Carlo calculations in Refs. [39,40].

of the quasiparticle interaction in both nuclear and neutron matter [1,41–43]. Recent auxiliary diffusion Monte Carlo calculations with realistic two- and three-nucleon forces find that the compressibility of neutron matter at the density $\rho = 0.16$ fm^{-3} is $\mathcal{K} \simeq 520$ MeV, approximately 50% larger than that of the noninteracting Fermi gas [14]. The isotropic component g_0 of the spin-spin interaction is enhanced by $\sim$15% at the resolution scale of 2.1 fm^{-1}, while the isotropic component h_0 of the exchange tensor interaction is reduced by a slightly smaller factor. The p-wave component f_1 of the spin-independent quasiparticle interaction increases as the resolution scale decreases. The corresponding values of the quasiparticle effective mass are $M^*/M_n = 0.78$ and 0.84 for the chiral and low-momentum interactions, respectively. In general our results from the low-momentum NN interaction agree qualitatively with those of Ref. [17], shown there (in dimensionless units) in the first three columns of Table I. We note that the different choice of low-momentum resolution scale in Ref. [17] accounts for some of the quantitative differences.

Next we compute the second-order particle-particle, hole-hole, and particle-hole diagrams, shown in Fig. 1, with two-neutron interactions. These provide the leading-order Pauli-blocking and polarization effects and give rise to components of the quasiparticle interaction depending explicitly on the center-of-mass momentum $\vec{P} = \vec{p}_1 + \vec{p}_2$. In Table V we display the Fermi liquid parameters associated with the second-order contributions (pp, hh and ph) for both the chiral N^{3}LO nucleon-nucleon interaction and the low-momentum interaction $V_{\text{low-k}}$ in neutron matter at a density ρ_0. Again we find in all cases good qualitative agreement between our results from the low-momentum NN interaction and the results of Table I in Ref. [17]. For the isotropic components, it is generally true that the particle-particle diagram gives contributions that are significantly larger than the hole-hole diagram. However, for higher values of L this is not the case, and the hole-hole diagram is in general comparable in magnitude to the particle-particle contribution. Coherent effects among the three diagrams are observed especially for the Landau parameters f_1, g_0, h_0, and k_0. Despite these large effects entering at second order, perturbative calculations of the equation of state of nuclear and neutron matter [44,45] show that third-order contributions should be significantly smaller. Second-order effects thus tend to dramatically increase the quasiparticle effective mass M^*, decrease the spin susceptibility of neutron matter and reduce the isotropic exchange tensor strength h_0. Although individually large, the contributions to f_0 nearly cancel at second order for the bare chiral NN interaction. With the low-momentum interaction the sum gives $f_0 = 0.379$ fm^2, which approximately cancels the reduction in f_0 from the renormalization group evolution at first order. The strong repulsion in the spin-independent channel from the particle-hole diagram is qualitatively similar to what has been found in previous Brueckner calculations of symmetric nuclear matter using hard-core interactions [41,42], where it was found that an infinite sum of polarization diagrams summed via the Babu-Brown–induced interaction [46,47] could stabilize nuclear matter against density fluctuations. In general, the particle-particle contributions decrease significantly in magnitude as the resolution scale is lowered. This effect is due primarily to the reduction in phase space in the particle-particle channel as the momentum cutoff is lowered. The results compiled in Table V were obtained with free-particle energies in the denominators of Eq. (12). In all subsequent tables, we include as well the one-loop corrections to the single-particle energies in the second-order diagrams (for details see Ref. [1]).

Finally, we calculate the contributions to the Fermi liquid parameters from the leading-order chiral three-neutron force. We evaluate the analytical formulas in Eqs. (54)–(59) for the central and exchange tensor contributions and perform numerical calculations of the cross-vector Fermi liquid parameters $l_L(k_f)$ in the standard representation given in

TABLE IV. The $L = 0, 1, 2, 3$ Fermi liquid parameters of the bare N^{3}LO chiral NN potential of Ref. [19] as well as the low-momentum NN potential $V_{\text{low-k}}$ at a resolution scale of 2.1 fm^{-1} at first order in many-body perturbation theory.

$k_f = 1.7$ fm^{-1}	Chiral N^{3}LO				$V_{\text{low-k}}^{(2.1)}$			
L	0	1	2	3	0	1	2	3
f [fm^2]	−0.700	−1.025	−0.230	−0.112	−1.188	−0.679	−0.298	−0.110
g [fm^2]	1.053	0.613	0.337	0.197	1.212	0.654	0.346	0.195
h [fm^2]	0.270	0.060	−0.040	−0.080	0.239	0.102	−0.051	−0.079

TABLE V. Second-order contributions to the $L = 0,\ 1,\ 2$ Fermi liquid parameters in neutron matter characterized by the Fermi momentum $k_f = 1.7$ fm^{-1}. We have separately listed the particle-particle (pp), hole-hole (hh), and particle-hole (ph) contributions for both the bare N^{3}LO chiral NN interaction as well as the low-momentum NN potential $V_{\text{low-k}}$ with $\Lambda_{\text{low-k}} = 2.1$ fm^{-1}.

$k_f = 1.7$ fm^{-1}		Chiral N^{3}LO			$V_{\text{low-k}}^{2.1}$		
L		0	1	2	0	1	2
f [fm^2]	pp	−0.773	0.547	−0.290	−0.225	0.042	−0.124
f [fm^2]	hh	−0.151	0.168	−0.121	−0.161	0.133	−0.063
f [fm^2]	ph	0.993	0.482	−0.089	0.765	0.795	0.255
Total		0.069	1.197	−0.500	0.379	0.970	0.068
g [fm^2]	pp	0.225	0.086	0.072	0.030	0.127	0.062
g [fm^2]	hh	0.006	0.089	−0.057	0.045	0.062	−0.059
g [fm^2]	ph	0.061	−0.016	−0.103	0.020	−0.011	−0.044
Total		0.293	0.159	−0.089	0.094	0.178	−0.040
h [fm^2]	pp	−0.101	0.112	−0.028	−0.047	0.042	−0.004
h [fm^2]	hh	−0.049	0.084	−0.049	−0.037	0.062	−0.032
h [fm^2]	ph	−0.062	−0.090	−0.066	−0.108	−0.116	−0.044
Total		−0.212	0.106	−0.143	−0.192	−0.012	−0.080
k [fm^2]	pp	−0.085	0.064	0.014	−0.057	0.037	0.010
k [fm^2]	hh	−0.036	0.052	−0.017	−0.028	0.039	−0.008
k [fm^2]	ph	−0.058	−0.017	0.075	−0.034	−0.019	0.042
Total		−0.178	0.098	0.072	−0.119	0.056	0.043
l [fm^2]	ph	0.135	−0.031	−0.279	−0.062	−0.147	−0.161

Eq. (60). In Fig. 5 we plot the density-dependent Fermi liquid parameters for the chiral three-neutron force with low-energy constants $c_1 = -0.81$ GeV^{-1} and $c_3 = -3.2$ GeV^{-1}. For densities larger than $\rho \simeq 0.5\rho_0$ the Landau parameters scale approximately linearly with the density. The largest effect is a strong additional repulsion in the isotropic spin-independent parameter f_0. In fact, at nuclear matter saturation density ρ_0, the strength of the three-body correction in this channel is larger than the two-neutron force contributions at 1st and 2nd order together. The quasiparticle effective mass M^*, governed by the parameter f_1, is reduced by less than 5% at saturation density ρ_0 with the inclusion of the two-pion exchange three-neutron force. Similar observations have been made in Ref. [2] for the case of symmetric nuclear matter where additional three-nucleon forces proportional to the low-energy constants c_4, c_D, and c_E are present. The qualitative similarities between the quasiparticle interaction in neutron matter and symmetric nuclear matter from three-body forces are due to the dominant role played by contributions proportional to the low-energy constant c_3 [2]. From the Landau parameters f_0 and f_1 we obtain for the compression modulus of neutron matter at $k_f = 1.7$ fm^{-1} the values $\mathcal{K} = 550$ and 660 MeV for the chiral and

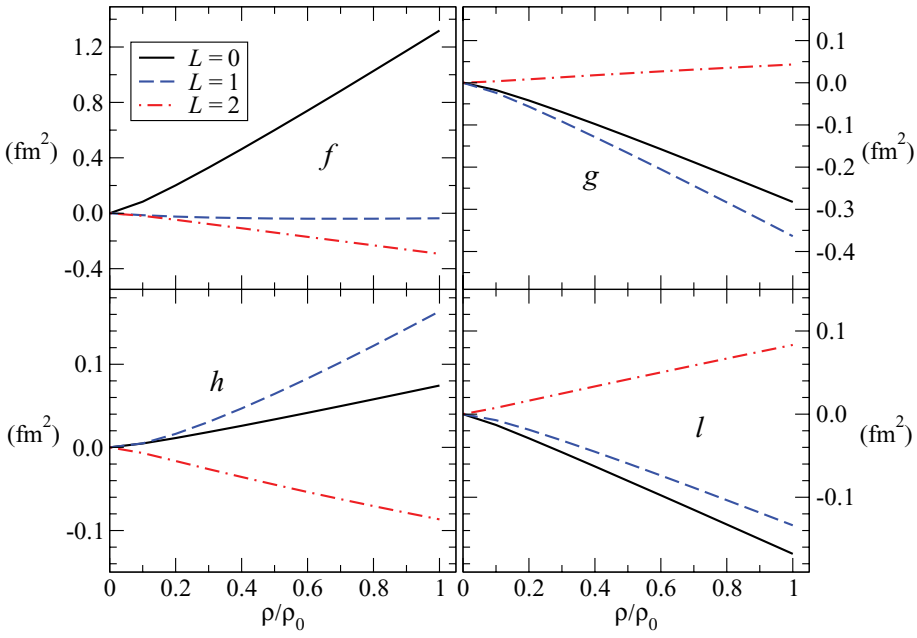

FIG. 5. (Color online) Density-dependent Fermi liquid parameters from the N^{2}LO chiral three-nucleon force for the quasiparticle interaction in neutron matter. The low-energy constants have the values $c_1 = -0.81$ GeV^{-1} and $c_3 = -3.2$ GeV^{-1}.

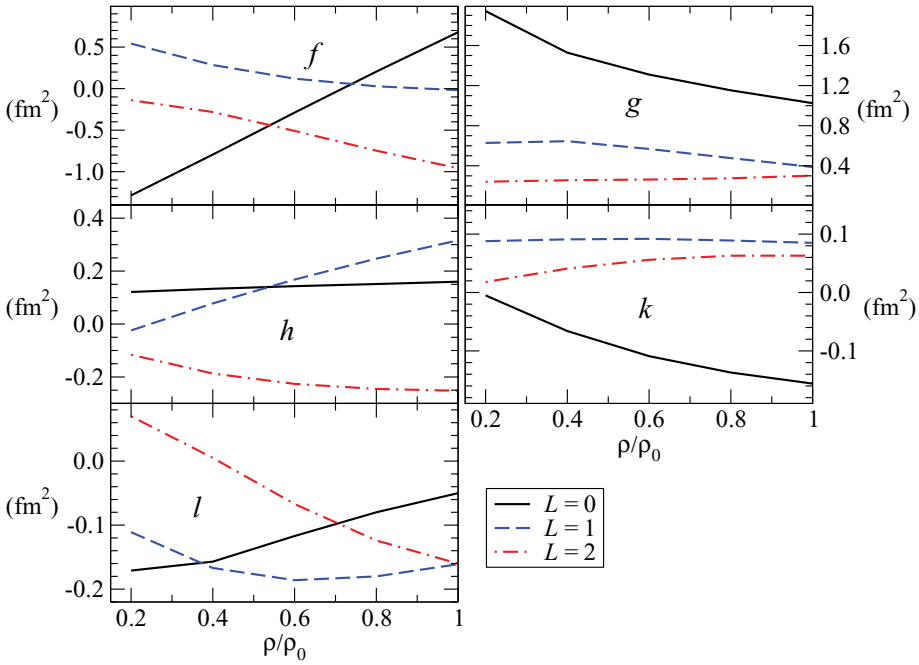

FIG. 6. (Color online) Density-dependent Fermi liquid parameters including first- and second-order contributions from the chiral N^{3}LO nucleon-nucleon potential of Ref. [19] as well as the N^{2}LO chiral three-nucleon force to leading order.

low-momentum potentials. These values compare well with those extracted numerically from the equation of state in Fig. 4. Neglecting effects from noncentral Fermi liquid parameters, the chiral three-neutron force at leading order tends to enhance the spin susceptibility χ of neutron matter [see Eq. (6)] by lowering g_0 by about 25% at ρ_0 from the value obtained with two-nucleon forces only. The three-body correction to the exchange tensor interaction is smaller in magnitude than the central force contributions. For the exchange tensor interaction the pion-self energy correction $V_{NN}^{\mathrm{med},1}$ and vertex correction $V_{NN}^{\mathrm{med},2}$ enter. As seen already in Ref. [2,32] both of these terms have the structure of one-pion exchange and are individually large with opposite sign. The cross-vector interaction from chiral three-nucleon forces is relatively small compared with the central quasiparticle interactions. However, at saturation density ρ_0 the magnitudes of the cross-vector Fermi liquid parameters l_0, l_1, and l_2 are comparable in magnitude to those from two-body potential at second order.

In Fig. 6 we combine the results for the first- and second-order two-body contributions with the leading-order three-body corrections at a resolution scale of $\Lambda = 2.5$ fm^{-1}. All Fermi liquid parameters up to $L = 2$ are plotted as a function of the neutron density ρ. The same quantities are compiled in Table VI at a Fermi momentum of $k_f = 1.7$ fm^{-1} together with the corresponding values from the low-momentum interaction $V_{\mathrm{low\text{-}k}}$ at the scale $\Lambda = 2.1$ fm^{-1}. From Fig. 6 one observes that all of the Fermi liquid parameters considered here for the spin-independent part of the quasiparticle interaction vary strongly with the density up to $\rho \simeq \rho_0$. In particular, the parameter f_0 has a nearly linear dependence on the density and gives rise to a compression modulus of neutron matter that grows strongly with increasing density. The Landau parameter f_1 decreases rapidly at small densities but flattens out close to nuclear matter saturation density, where it nearly vanishes thereby yielding an effective mass $M^*/M_n \simeq 1$ according to Eq. (5). The $L = 2$ component of the spin-independent quasiparticle interaction exhibits a nearly linear decrease with the neutron density, and owing to coherent effects from all contributions it attains a large negative value at and beyond saturation density. From Table VI we see that this is a scale-independent prediction that to our knowledge has not been previously observed in the literature. In fact, such a large negative value could help in fulfilling the forward scattering Pauli principle sum rule, which in the absence of noncentral interactions takes the form

$$\sum_{L=0}^{\infty}\left[\frac{F_L}{1+F_L/(2L+1)}+\frac{G_L}{1+G_L/(2L+1)}\right]=0. \quad (68)$$

The presence of noncentral interactions modifies this sum rule [48], but the effect of center-of-mass tensor and cross-vector interactions has not yet been explored.[1] The isotropic component g_0 of the spin-spin quasiparticle interaction decreases with neutron density. For densities larger than ρ_0, the density dependence of g_0 is governed mainly by the three-neutron force contributions, which decrease g_0 and consequently increase the neutron matter spin susceptibility χ. Considering only central interactions we find no evidence for a phase transition to a ferromagnetic state (characterized by $G_0 = N_0 g_0 \leqslant -1$) close to nuclear matter saturation density. The additional noncentral interactions considered in the present work are expected to modify the general stability conditions for Fermi liquids [49], but to date the effects of neither the center-of-mass tensor nor cross-vector interactions have been included. The isotropic component h_0 of the exchange tensor interaction is nearly independent of the density, since the medium corrections from two- and three-body forces approximately cancel. The Fermi liquid parameters of the

[1]Furthermore, a vanishing forward scattering amplitude in odd partial waves may require a large number of Fermi liquid parameters, as we discuss in Appendix B.

TABLE VI. Fermi liquid parameters for the quasiparticle interaction in neutron matter at a density corresponding to a Fermi momentum of $k_f = 1.7$ fm^{-1}. The low-energy constants of the N^{2}LO chiral three-nucleon force are chosen to be $c_1 = -0.81$ GeV^{-1} and $c_3 = -3.2$ GeV^{-1} when employed together with the bare chiral NN interaction and $c_1 = -0.76$ GeV^{-1} and $c_3 = -4.78$ GeV^{-1} with the low-momentum interaction $V_{\text{low-k}}$.

$k_f = 1.7$ fm^{-1}	Chiral N^{3}LO			$V_{\text{low-k}}^{2.1}$		
L	0	1	2	0	1	2
f [fm^2]	0.679	−0.018	−0.959	1.072	0.135	−0.686
g [fm^2]	1.025	0.388	0.302	0.880	0.298	0.380
h [fm^2]	0.160	0.316	−0.252	0.175	0.317	−0.263
k [fm^2]	−0.156	0.085	0.063	−0.108	0.051	0.039
l [fm^2]	−0.050	−0.161	−0.160	−0.295	−0.330	−0.029

novel center-of-mass tensor and cross-vector interactions are relatively small in magnitude, but k_0, l_0, and l_2 have a strong density dependence. From Table VI we see that there remains a moderate dependence on the resolution scale and choice of low-energy constants. These variations lead to differences on the order of 10%–30% for most of the $L = 0, 1, 2$ Fermi liquid parameters.

VI. CONCLUSIONS AND OUTLOOK

In the present work we have computed the $L = 0, 1, 2$ Fermi liquid parameters for the quasiparticle interaction in neutron matter employing realistic two- and three-nucleon interactions derived within chiral effective-field theory. In addition to the free-space contribution from the two-body interaction, we have calculated without any simplifying approximations the second-order two-body correction as well as the leading three-body correction. A general method for extracting all components of the quasiparticle interaction, both central and noncentral parts, for two-body interactions given in a partial-wave representation has been developed and tested with simple model interactions that can be treated semi-analytically. Employing realistic two- and three-neutron forces, we find that medium-dependent loop corrections play an important role in increasing the compression modulus of neutron matter from an unphysically small value to about $\mathcal{K} = 600$ MeV at nuclear matter saturation density ρ_0. Second-order effects from two-body forces strongly enhance the quasiparticle effective mass M^*, while three-neutron forces play only a minor role for this quantity. The first- and second-order contributions to g_0 from two-body forces are positive for the densities considered in the present work, although they decrease in magnitude for increasing density. When combined with the medium-dependent loop corrections from the leading-order chiral three-neutron forces, the Landau parameter g_0 decreases with density, which in the absence of noncentral interactions would lead to an increasing spin susceptibility χ of neutron matter. The noncentral components of the quasiparticle interaction h_L, k_L, and l_L have been computed as a function of the neutron density ρ. The extent to which they affect the spin susceptibility of neutron matter as well as the response functions for electroweak probes will be studied in future work.

ACKNOWLEDGMENTS

Work was supported in part by BMBF, the DFG cluster of excellence Origin and Structure of the Universe, by the DFG, NSFC (CRC110), and US DOE Grant No. DE-FG02-97ER-41014.

APPENDIX A: ENERGY PER PARTICLE FROM MODEL INTERACTIONS AT SECOND ORDER

Organizing the second-order calculation of the energy density $\rho\bar{E}$ in the number of medium insertions [see Eq. (22)], one must evaluate (two-ring) Hartree and (one-ring) Fock diagrams each with two or three medium insertions. We give first the pertinent analytical expressions for the pseudoscalar interaction in Eq. (23) at second order.

Hartree diagram with two medium insertions:

$$\bar{E}(k_f)^{(H2)} = \frac{g^4 M_n}{(8\pi)^3}\left\{\frac{21}{2u} - 15u + 32\arctan 2u - \frac{7}{8u^3}(3+20u^2)\ln(1+4u^2)\right\}. \quad \text{(A1)}$$

Fock diagram with two medium insertions:

$$\bar{E}(k_f)^{(F2)} = \frac{g^4 M_n}{(4\pi u)^3}\left\{2u^2 - 7u^3\arctan u + 6\sqrt{2}u^3\arctan(\sqrt{2}u) + \left(1+\frac{9u^2}{2}\right)\ln(1+u^2) - 3\left(\frac{1}{2}+2u^2\right)\ln(1+2u^2) + 4\int_0^u dx\, x(u-x)^2(2u+x)\frac{1+4x^2+8x^4}{(1+2x^2)^3}(\arctan x - \arctan 2x)\right\}. \quad \text{(A2)}$$

Hartree diagram with three medium insertions:

$$\bar{E}(k_f)^{(H3)} = \frac{g^4 M_n}{32\pi^4 u^3}\int_0^u dx\, x^2\int_{-1}^1 dy\left[2uxy + (u^2 - x^2y^2)\ln\frac{u+xy}{u-xy}\right]\frac{s^6}{(1+s^2)^3}. \quad \text{(A3)}$$

Fock diagram with three medium insertions:

$$\bar{E}(k_f)^{(F3)} = \frac{3g^4 M_n}{64\pi^4 u^3}\int_0^u dx\Bigg\{-2\left[u - \frac{1+u^2+x^2}{4x}\ln\frac{1+(u+x)^2}{1+(u-x)^2}\right]^2 + x^2\int_{-1}^1 dy\int_{-1}^1 dz\frac{yz\theta(y^2+z^2-1)}{|yz|\sqrt{y^2+z^2-1}}\left[\ln(1+s^2)-\frac{s^2}{1+s^2}\right]\left[\ln(1+t^2)-\frac{t^2}{1+t^2}\right]\Bigg\}, \tag{A4}$$

with abbreviations $u = k_f/m$, $s = xy + \sqrt{u^2 - x^2 + x^2y^2}$, and $t = xz + \sqrt{u^2 - x^2 + x^2z^2}$.

For the spin-orbit interaction [Eq. (38)] at second order the analogous expressions read

$$\bar{E}(k_f)^{(H2)} = \frac{g_s^4 M_n}{(4\pi)^3}\left\{\frac{5u}{2} - \frac{2u^3}{3} - \frac{3}{4u} - 4\arctan 2u + \frac{3+28u^2}{16u^3}\ln(1+4u^2)\right\}, \tag{A5}$$

$$\bar{E}(k_f)^{(F2)} = \frac{g_s^4 M_n}{(2\pi u)^3}\left\{\frac{u^2}{2} - 4u^3\arctan u + 3\sqrt{2}u^3\arctan(\sqrt{2}u) + (1+3u^2)\ln(1+u^2) - 3\left(\frac{1}{4}+u^2\right)\ln(1+2u^2) + 2\int_0^u dx x(u-x)^2(2u+x)\frac{1+4x^2+8x^4}{(1+2x^2)^3}(\arctan x - \arctan 2x)\right\}, \tag{A6}$$

$$\bar{E}(k_f)^{(H3)} = \frac{g_s^4 M_n}{64\pi^4 u^3}\int_0^u dx x^2\int_{-1}^1 dy \times\left[2uxy\left(\frac{5u^2}{3}+2x^2-3x^2y^2\right) + (u^2-x^2y^2)(u^2+2x^2-3x^2y^2)\times\ln\frac{u+xy}{u-xy}\right]\frac{s^4(3+s^2)}{(1+s^2)^3}, \tag{A7}$$

$$\bar{E}(k_f)^{(F3)} = \frac{3g_s^4 M_n}{16\pi^4 u^3}\int_0^u dx \times\Bigg\{-\left[u - \frac{1+u^2+x^2}{4x}\ln\frac{1+(u+x)^2}{1+(u-x)^2}\right]^2 + x^2\int_{-1}^1 dy\int_{-1}^1 dz\frac{yz\theta(y^2+z^2-1)}{|yz|\sqrt{y^2+z^2-1}} \times\left[\ln(1+s^2)-\frac{s^2}{1+s^2}\right] \times\left[\ln(1+t^2)-\frac{t^2}{1+t^2}\right]\Bigg\}, \tag{A8}$$

where $u = k_f/m_s$. An interesting feature of the second-order spin-orbit interaction is that for large mass m_s the Hartree and Fock contributions become equal with the same sign. It is worth noting that the agreement between these semi-analytic results and those based on the partial-wave decomposition (66) agree on the per mille level.

APPENDIX B: FORWARD SCATTERING AMPLITUDES FOR MODEL INTERACTIONS AND CHIRAL THREE-NUCLEON FORCE

The forward scattering amplitude for two quasiparticles on the Fermi surface receives the following contribution from pseudoscalar boson exchange (23) at second order in many-body perturbation theory:

$$\mathcal{F}(\vec{p}_1,\ \vec{p}_1) = (1-\vec{\sigma}_1\cdot\vec{\sigma}_2)\frac{g^4 M_n}{64\pi^2 m^3} \times\left\{\arctan 2u - \frac{\pi}{2} - \frac{2u(3+20u^2)}{3(1+4u^2)^2}\right\}, \tag{B1}$$

with $u = k_f/m$, while one gets from a scalar boson exchange, $V_C(q) = -g^2/(m^2+q^2)$, at second order:

$$\mathcal{F}(\vec{p}_1,\ \vec{p}_1) = (1-\vec{\sigma}_1\cdot\vec{\sigma}_2)\frac{g^4 M_n}{16\pi^2 m^3}(2\arctan 2u - \pi). \tag{B2}$$

The spin-orbit interaction (38) at second order leads in fact to a vanishing contribution to $\mathcal{F}(\vec{p}_1,\ \vec{p}_1)$. Furthermore, the N^{2}LO chiral three-neutron interaction treated at first order gives rise to a quasiparticle forward scattering amplitude of the form

$$\mathcal{F}(\vec{p}_1,\ \vec{p}_1) = (1-\vec{\sigma}_1\cdot\vec{\sigma}_2)\frac{g_A^2 m_\pi^3}{16\pi^2 f_\pi^4}\left\{4u(c_3-c_1) - \frac{4c_3u^3}{3} + (6c_1-5c_3)\arctan 2u + \frac{3c_3-4c_1}{2u} \times\ln(1+4u^2)\right\}, \tag{B3}$$

TABLE VII. Values of S_n (divided by S_0) at $u = 2.48$ for various increasing n.

n	S_n/S_0
5	0.23
10	0.04
15	0.006
20	0.0001

with $u = k_f/m_\pi$. We note that in all of these cases only the central components of the quasiparticle scattering amplitude remain in the forward limit $\vec{p}_2 \to \vec{p}_1$. The important feature about these forward scattering amplitudes is their proportionality to the operator $(1 - \vec{\sigma}_1 \cdot \vec{\sigma}_2)$. It makes them vanish identically in the spin-triplet state as required by the Pauli principle.

Next, we investigate the convergence of the Legendre polynomial expansion of the quasiparticle interaction in the simple case of one-pion exchange. The obvious vanishing of one-pion exchange in forward direction ($\vec{q} = 0$) implies that the following sequence converges to zero:

$$S_n = \sum_{L=0}^{n} (2L+1) \int_{-1}^{1} dz P_L(z) \frac{u^2(1-z)}{1+2u^2(1-z)}, \quad \text{(B4)}$$

with $u = k_f/m_\pi$ and the prefactor from coupling constants has been omitted. Choosing $k_f = 1.7$ fm^{-1}, we list in Table VII the values of S_n (divided by S_0) at $u = 2.48$ for various increasing n.

One observes from this example that in practice satisfying the Pauli principle zero sum rule with good accuracy will be delicate and requires knowledge of a large number of Landau parameters.

[1] J. W. Holt, N. Kaiser, and W. Weise, Nucl. Phys. A **870-871**, 1 (2011).
[2] J. W. Holt, N. Kaiser, and W. Weise, Nucl. Phys. A **876**, 61 (2012).
[3] A. Leggett, Phys. Rev. **147**, 119 (1966).
[4] L. B. Leinson, Phys. Rev. C **79**, 045502 (2009).
[5] M. E. Gusakov, Phys. Rev. C **81**, 025804 (2010).
[6] N. Iwamoto and C. J. Pethick, Phys. Rev. D **25**, 313 (1982).
[7] J. Navarro, E. S. Hernández, and D. Vautherin, Phys. Rev. C **60**, 045801 (1999).
[8] G. I. Lykasov, C. J. Pethick, and A. Schwenk, Phys. Rev. C **78**, 045803 (2008).
[9] S. Bacca, K. Hally, C. J. Pethick, and A. Schwenk, Phys. Rev. C **80**, 032802 (2009).
[10] P. Haensel and A. J. Jerzak, Phys. Lett. B **112**, 285 (1982).
[11] E. Olsson, P. Haensel, and C. J. Pethick, Phys. Rev. C **70**, 025804 (2004).
[12] M. A. Pérez-García, J. Navarro, and A. Polls, Phys. Rev. C **80**, 025802 (2009).
[13] C. J. Pethick and A. Schwenk, Phys. Rev. C **80**, 055805 (2009).
[14] S. Fantoni, A. Sarsa, and K. E. Schmidt, Phys. Rev. Lett. **87**, 181101 (2001).
[15] A. Rios, A. Polls, and I. Vidaña, Phys. Rev. C **71**, 055802 (2005).
[16] P. Haensel and J. Dabrowski, Nucl. Phys. A **254**, 211 (1975).
[17] A. Schwenk and B. Friman, Phys. Rev. Lett. **92**, 082501 (2004).
[18] N. Kaiser, Nucl. Phys. A **768**, 99 (2006).
[19] D. R. Entem and R. Machleidt, Phys. Rev. C **68**, 041001(R) (2003).
[20] E. Epelbaum, Prog. Part. Nucl. Phys. **57**, 654 (2006).
[21] D. Gazit, S. Quaglioni, and P. Navrátil, Phys. Rev. Lett. **103**, 102502 (2009).
[22] S. K. Bogner, T. T. S. Kuo, and A. Schwenk, Phys. Rep. **386**, 1 (2003).
[23] S. K. Bogner, R. J. Furnstahl, and A. Schwenk, Prog. Part. Nucl. Phys. **65**, 94 (2010).
[24] L. D. Landau, Sov. Phys. JETP **3**, 920 (1957); **5**, 101 (1957); **8**, 70 (1959).
[25] G. Baym and C. Pethick, *Landau Fermi-Liquid Theory* (Wiley & Sons, New York, 1991).
[26] A. B. Migdal, *Theory of Finite Fermi Systems and Applications to Atomic Nuclei* (Interscience, New York, 1967).
[27] A. A. Abrikosov and I. M. Khalatnikov, Rep. Prog. Phys. **22**, 329 (1959).
[28] S. K. Bogner, T. T. S. Kuo, L. Coraggio, A. Covello, and N. Itaco, Phys. Rev. C **65**, 051301(R) (2002).
[29] A. Nogga, S. K. Bogner, and A. Schwenk, Phys. Rev. C **70**, 061002(R) (2004).
[30] M. C. M. Rentmeester, R. G. E. Timmermans, and J. J. de Swart, Phys. Rev. C **67**, 044001 (2003).
[31] J. W. Holt, N. Kaiser, and W. Weise, Phys. Rev. C **79**, 054331 (2009).
[32] J. W. Holt, N. Kaiser, and W. Weise, Phys. Rev. C **81**, 024002 (2010).
[33] K. Hebeler and A. Schwenk, Phys. Rev. C **82**, 014314 (2010).
[34] A. Akmal, V. R. Pandharipande, and D. G. Ravenhall, Phys. Rev. C **58**, 1804 (1998).
[35] R. B. Wiringa, V. G. J. Stoks, and R. Schiavilla, Phys. Rev. C **51**, 38 (1995).
[36] R. B. Wiringa, S. C. Pieper, J. Carlson, and V. R. Pandharipande, Phys. Rev. C **62**, 014001 (2000).
[37] N. Kaiser, Eur. Phys. J. A **48**, 36 (2012).
[38] I. Tews, T. Krueger, K. Hebeler, and A. Schwenk, Phys. Rev. Lett. **110**, 032504 (2013).
[39] P. Armani, A. Y. Illarionov, D. Lonardoni, F. Pederiva, S. Gandolfi, K. Schmidt, and S. Fantoni, J. Phys.: Conf. Ser. **336**, 012014 (2011).
[40] S. Gandolfi, A. Y. Illarionov, K. E. Schmidt, F. Pederiva, and S. Fantoni, Phys. Rev. C **79**, 054005 (2009).
[41] O. Sjöberg, Ann. Phys. (NY) **78**, 39 (1973).
[42] O. Sjöberg, Nucl. Phys. A **209**, 363 (1973).
[43] J. W. Holt, G. E. Brown, J. D. Holt, and T. T. S. Kuo, Nucl. Phys. A **785**, 322 (2007).
[44] K. Hebeler, S. K. Bogner, R. J. Furnstahl, A. Nogga, and A. Schwenk, Phys. Rev. C **83**, 031301 (2011).
[45] L. Coraggio, J. W. Holt, N. Itaco, R. Machleidt, and F. Sammarruca, arXiv:1209.5537 [Phys. Rev. C (to be published)].
[46] S. Babu and G. E. Brown, Ann. Phys. (NY) **78**, 1 (1973).
[47] S. O. Bäckman, G. E. Brown, and J. A. Niskanen, Phys. Rep. **124**, 1 (1985).
[48] B. L. Friman and A. K. Dhar, Phys. Lett. B **85**, 1 (1979).
[49] S.-O. Bäckman, O. Sjöberg, and A. D. Jackson, Nucl. Phys. A **321**, 10 (1979).